Novel Physiological Function of the Cellular Prion Protein (PrP^C) in Exosomal Trafficking

Dissertation

Zur Erlangung der Würde des Doktors der Naturwissenschaften

Des Fachbereichs Biologie, der Fakultät für Mathematik, Informatik und Naturwissenschaften, der Universität Hamburg
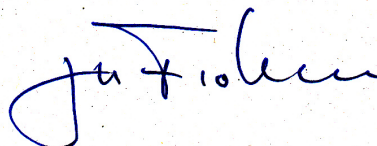

vorgelegt von

Dana Kathrin Thurm

aus Duisburg

Hamburg 2012

Genehmigt vom Fachbereich Biologie
der Fakultät für Mathematik, Informatik und Naturwissenschaften
an der Universität Hamburg
auf Antrag von Professor Dr. M. Glatzel
Weitere Gutachterin der Dissertation:
Priv.-Doz. Dr. S. Lüthje
Tag der Disputation: 17. Februar 2012

Hamburg, den 02. Februar 2012

Professor Dr. J. Fromm
Vorsitzender des Promotionsausschusses
Biologie

Yale University

Laura Swan, Ph.D.

Department of Cell Biology
295 Congress Ave.
BCMM 237
New Haven, Connecticut
06520-2137
Telephone: 203 737-4469
e-mail: laura.swan@yale.edu

16 December 2011

TO WHOM IT MAY CONCERN

Dear Sir/Madam:

I am a native English Speaker. I have read the PhD thesis submitted by Mrs. Dana Kathrin Thurm and herby confirm that it complies with the rules of the English language.

Yours Sincerely,

Laura Swan

TABLE OF CONTENTS

1 ABSTRACT

The cellular prion protein (PrP^C) is a cell-surface glycoprotein, predominantly expressed in neurons and in lymphoid tissue. In prion diseases, misfolding of PrP^C to PrP^{Sc} constitutes a central element of disease pathogenesis and PrP^{Sc} is an essential component of the transmissible agent. PrP^C is postulated to be involved in several physiological processes such as signalling and phagocytosis, but the exact mechanisms are poorly understood. Physiological active PrP^C is transported between cells and between tissues while the trafficking of PrP^{Sc} propagates conversion of PrP^C to PrP^{Sc} throughout an organism resulting in PrP^{Sc} accumulation in the brain leading to prion disease. Both conformers are transported via exosomes, which are small vesicles released by various cell types including immune cells and neurons. We hypothesise a role for PrP^C in exosomal trafficking. Since endocytic compartments represent an important step in phagocytosis, signalling, and conversion of PrP^C to PrP^{Sc}, we addressed internalization of exosomes by neuronal cells. To identify PrP^C-dependent alterations in exosomal uptake efficiencies we established a new assay allowing quantification of exosomes and their internalization. We demonstrated a strong decrease of exosomal uptake due to the presence of PrP^C on exosomes or plasma membrane of neuronal recipient cells (cell lines and primary neurons). Furthermore PrP^C retains exosomes in early recycling compartments while the absence of PrP^C results in transport of exosomes towards lysosomes. These findings indicate a novel physiological function of PrP^C in regulating exosomal uptake and may provide an explanation for reduced immune activation and increased phagocytosis in prion knockout mice as well as for the highly efficient spread of PrP^{Sc} via exosomes.

2 INTRODUCTION

2.1 The Prion Protein (PrP)

The cellular prion protein (PrP^C) is highly conserved throughout evolution. In mammals, where aminoacid sequence homology is particularly high, PrP^C is expressed ubiquitously with high levels found in the central nervous system (CNS) (Spielhaupter and Schatzl 2001). PrP^C is encoded within the chromosomal *Prnp* gen (McKnight, Alexander et al. 1986). The 254 aminoacid-long pre protein (253 in humans) contains a signal sequence for targeting to the secretory pathway, a five-octarepeat-region near the N-terminus, two glycosylation sites at asparagine 180 and 196 (Caughey, Race et al. 1989; Haraguchi, Fisher et al. 1989), a single disulphide bridge (AA 179 to 214), and a region coding for a glycosylphosphatidylinositol-anchor (GPI-anchor) (Fig. 2.1). Following biogenesis, PrP^C is transported to the cell surface where it is held in the outer leaflet of the plasma membrane by the GPI-anchor, where it is thought to be associating with cholesterol-rich raft membrane subdomains. On the plasma membrane the un-, mono, and diglycosylated forms PrP^C are found.
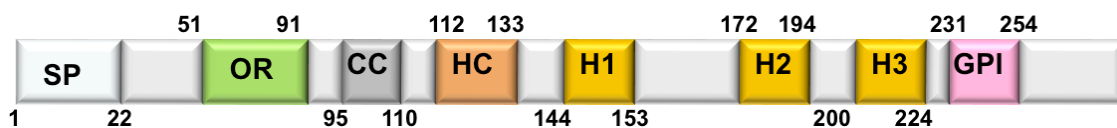
Figure 2.1: Functional domains of mouse PrP^C.
SP= signal peptide, OR= Octarepeat, CC= charged core, HC= hydrophobic core, H1-3= α-helices 1-3; GPI= GPI-anchor

2.2   Physiological function of the cellular Prion Protein (PrP^C)

Consistent with a high degree of sequence identity, the globular half of PrP^C is structured the same manner in mammals. Interestingly, even in non-mammalian PrP^C which has low sequence identity, a certain preservation of structure was found (Calvete, Solis et al. 1994) pointing to an important function for PrP^C through evolution. With the intention to examine this physiological function, transgenic mice have been generated where the *Prnp* gene was knocked out (PrP$^{0/0}$). Knocking out PrP^C was nonlethal, and these mice displayed a normal behaviour, with exception of their resistance to prion infection, as they do not contain any PrP^C which could be converted to PrP^{Sc} (Bueler, Fischer et al. 1992; Bueler, Aguzzi et al. 1993). These PrP$^{0/0}$ mice have become a common tool in research on PrP^C, especially of its

physiological function. PrP^C is present in many tissues and components of the immune system and in peripheral organs (Cashman, Loertscher et al. 1990; Manson, West et al. 1992; Horiuchi, Yamazaki et al. 1995; Brown, Schmidt et al. 1998; Dodelet and Cashman 1998; Durig, Giese et al. 2000; Kubosaki, Yusa et al. 2001; Li, Liu et al. 2001). It is predominantly expressed in neurons of the brain and the peripheral nervous system (Hay, Barry et al. 1987). Therefore the function of PrP^C in the nervous system has been examined revealing a role of PrP^C in behaviour (adaption to stress) (Nico, de-Paris et al. 2005), circadian rhythm regulation (Fischer, Rulicke et al. 1996; Tobler, Gaus et al. 1996), memory, and neuronal excitability (Nishida, Katamine et al. 1997; Maglio, Perez et al. 2004). PrP^C has also been shown to be involved in the modulation of phagocytosis and autophagy (de Almeida, Chiarini et al. 2005; Oh, Shin et al. 2008).
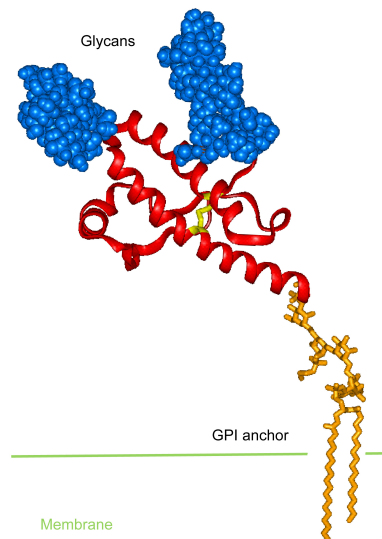
Figure 2.2: Cellular PrP (PrP^C) at the plasma membrane.
Panel shows diglycosylated (polysaccharides indicated in blue) PrP^C held anchored to plasma membrane via a glycosylphosphatidyl-anchor (yellow). The N terminus (α-helices and loops indicated in red, β-strands in blue) is highly flexible and can interact with proteins. Mono- and unglycosylated forms of PrP^C are also present at the plasma membrane. Figure modified after Rea
(http://www.bris.ac.uk/biochemistry/research/rs.html).

2.3 The Prion Principle

The same single-copy gene encoding for PrP^C also encodes PrP^{Sc}, an anomalous conformational isoform of PrP^C with an identical primary structure, but with different posttranslational modifications. The estimated structure of PrP^C consists of a globular domain made of three α-helices (in human) interspersed with two short antiparallel β-strands (Fig. 2.3) (Riek, Hornemann et al. 1996; James, Liu et al. 1997; Riek, Wider et al. 1998; Zahn, Liu et al. 2000). When the precursor protein is converted into

PrP^{Sc} it becomes enriched in β- sheets and undergoes changes in posttranslational modifications (Colby and Prusiner 2011). Due to these structural differences, PrP^{Sc} is highly resistant to proteinase digestion, detergents, and phospholipase C, which cleaves the GPI-anchor on PrP^C (Stimson, Hope et al. 1999; Chiesa, Piccardo et al. 2003; Stohr, Elfrink et al. 2011) (Hsiao 1994; Gambetti, Dong et al. 2008). Interestingly, the degree of resistance differs for the various PrP^{Sc} strains observed.
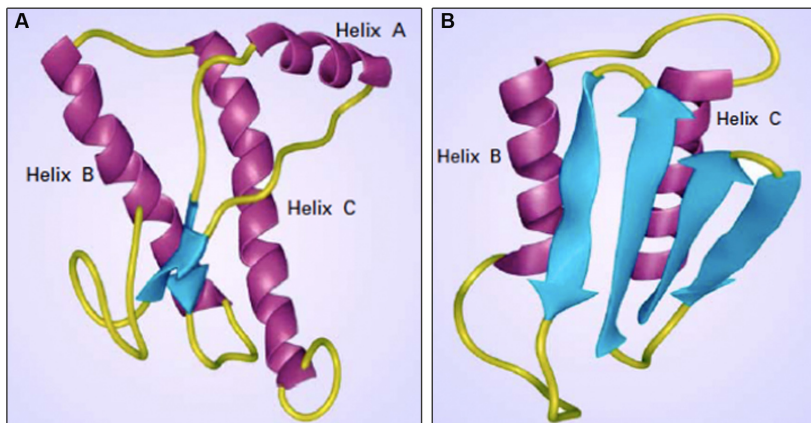
Figure 2.3: Predicted structures of the prion protein (PrP) conformers.
The structure of Syrian hamster recombinant PrP 90-231 presumably resembles that of the cellular isoform (PrP^C). It consists of 3 α-helices (Helix A, residues 144 through 157; Helix B, 172 through 193, and Helix C, 200 through 277) indicated in purple. Loops are indicated in yellow and blue represents β-strands (A). The predicted tertiary structure of human PrP^{Sc} exhibits 4 β-strands (blue), S1 β-strands (residues 108 through 113 and 116 through 122) and S2 β-strands (125 through 135 and 138 through 144). It bears 2 α-helices (Helix B, 178 through 191 and Helix C, residues 202 through 218) indicated in purple, with yellow loops (B). Figure modified after Prusiner. (Prusiner 2001)

Prion propagation requires posttranslational conversion of PrP^C into the infectious conformation PrP^{Sc}, which was discovered in Scrapie infected sheep for the first time by S. Prusiner (1982). After initial formation of PrP^{Sc} due to an incompletely understood mechanism or following infection with infectious prions, PrP^{Sc} acts as a template for conversion at the expense of PrP^C (Huang, Gabriel et al. 1994). The exact mechanism of conformational change is not known yet, but prions are thought to amplify in a self-catalytic misfolding process, which strictly depends on the presence of PrP^C (Büeler, Aguzzi et al. 1993). Investigations on prion conversion *in vitro* and *in vivo* indicate that an intermediate, partially unfolded state of PrP is necessary to achieve prion conversion (Cohen 1994; Kocisko, Come et al. 1994; Kaneko, Zulianello et al. 1997; Castilla, Saa et al. 2005). Furthermore, in studies on cell-free systems PrP^{Sc} was able to cause PrP^C to convert into a proteinase resistant

isoform. This conversion process is highly dependent on species and sequence homology, consistent with the observed species barriers *in vivo* (Kocisko, Come et al. 1994; Bessen, Kocisko et al. 1995; Raymond, Hope et al. 1997; Hill, Butterworth et al. 1999). The conversion mechanism is thought to require template-seeded polymerisation and to be independent of nucleic acid and thus, the conversion might be managed in a non-catalytic or autocatalytic way (Gajdusek 1988; Jarrett and Lansbury 1993; Caughey, Kocisko et al. 1995). In scrapie-infected cells, PrP^{Sc} multimers might act as the seed of conversion and directly convert host-PrP^{C} (Callahan, Xiong et al. 2001; Caughey, Raymond et al. 2001; Silveira, Raymond et al. 2005). Interestingly, several lines of evidence indicate that this PrP^{C} conversion into PrP^{Sc} takes place mainly in recycling endosomal compartments (Borchelt, Taraboulos et al. 1992; Marijanovic, Caputo et al. 2009).

When transgenic mice highly overexpressing a truncated fragment of recombinant PrP^{C} (PrP90-231) were inoculated with synthetic amyloid fibrils built by the PrP90-231 fragment, clinical disease could be observed and the inoculation with brain tissue of these mice could even spread infection to wild type mice (Legname, Baskakov et al. 2004; Legname, Nguyen et al. 2005).

Based on *in vitro* experiments, the existence of a possible cofactor is discussed, which might mediate the interaction of PrP^{C} and PrP^{Sc} and therefore enhance the conversion to the pathogenic isoform (Raeber, Sailer et al. 1999; Deleault, Harris et al. 2007; Wang, Zhou et al. 2010). So far, no concrete cofactor could be identified, although it seems that some factors, such as cell- or tissue-specific regulatoion of PrP^{C} expression, genetic alterations, environmental factors, and co incubation of PrP^{C} with stimulatory polyanionic compounds might alter the probability of PrP^{C} conversion to PrP^{Sc} (Telling, Scott et al. 1995; Saborio, Soto et al. 1999; Stephenson, Chiotti et al. 2000; Lloyd, Onwuazor et al. 2001; Manolakou, Beaton et al. 2001; Deleault, Geoghegan et al. 2005; Safar, Lessard et al. 2008).

2.4 Prion diseases

Several Prion diseases are known to affect humans and animals. They can occur sporadically, because of genetic origin or due to infection like in Transmissible Spongiform Encephalopathies (TSEs) (Prusiner and Scott 1997; Prusiner, Scott et al. 1998). After a long incubation time of several years or decades, symptoms like seizures, and ataxia will occur. Patients will lose their motor and cognitive abilities,

showing loss of memory and dementia. All known Prion diseases are lethal. Morphologically, they are characterised by neuropathological features such as spongiform changes in the grey matter of the cerebellum, amyloid plaques, neuronal loss, and astrocytic activation (gliosis) in the CNS (Klatzo, Gajdusek et al. 1959; Wille, Baldwin et al. 1996; Mallucci, Campbell et al. 1999). These features occur due to accumulations of fibrils and cross-β-core PrP^{Sc} structures, called amyloids, in the brain. This Proteinaceous infectious particle (Prion) is highly resistant to heat and disinfection (Steelman 1994) and can be transmitted via different routes, such as oral uptake, neurosurgical interventions, hormone substitution or blood transfusion (Bruce, Will et al. 1997; Hill, Desbruslais et al. 1997; Brown, Preece et al. 2000; Hunter, Foster et al. 2002; Baier, Norley et al. 2003; Peden, Head et al. 2004). Following the "protein-only-hypothesis," this pathogenic conformer of PrP^{C} is the only causative agent of Prion diseases (1991). The most common Prion disease in humans is the Creutzfeldt-Jakob disease (CJD), which can appear in four different forms; the sporadic, variant, genetic and iatrogenic CJD. The most prominent form is the sporadic CJD (sCJD), representing approximately 85% of all cases. The exact origin of this disease is still under discussion, but a spontaneous misfolding of PrP^{C} into PrP^{Sc} is hypothesised (Hsiao, Scott et al. 1991). Gnetic prion diseases, such as Gerstmann-Sträussler-Scheinker syndrome (GSS), Fatal Familiar Insomnia (FFI), and genetic Creutzfeldt-Jakob disease (gCJD) are neurodegenerative diseases, which are caused by *PRNP* mutations favouring the conversion of the PrP^{C} into the prion state (PrP^{Sc}), and account for approximately 10% of human prion diseases (Roos, Gajdusek et al. 1973; Hsiao, Baker et al. 1989; Prusiner 1989; Kovacs, Hoftberger et al. 2005). In other mammals Prion diseases have been observed as well, such as Scrapie in sheep and goats, transmissible mink encephalopathy (TME) in mink, feline spongiform encephalopathy, chronic wasting disease (CWD) in deer and elk, and Bovine Spongiform Encephalopathy (BSE) in cattle (Johnson 2005; Mackay, Knight et al. 2011). The mean incubation time has been shown to be strain specific, but it usually takes several years. For instance, it takes approximately 5 years for BSE (Stekel, Nowak et al. 1996). Considering the different PrP^{Sc} strains isolated from infected animals, a species barrier of transmission has been discussed (Bruce, Chree et al. 1994; Billeter, Riek et al. 1997). However, contrary to this species barrier, PrP^{Sc} infection could be transmitted from CJD and GSS in humans and BSE in cattle experimentally to hamster and mice (Weissmann 1991; Bruce,

Chree et al. 1994) and with a low transfection rate CWD prions could transmit infection to cattle after intracerebral inoculation (Hamir, Cutlip et al. 2001).

2.5 Transport of PrP^C and PrP^{Sc}

PrP^C is a ubiquitous cell-surface glycoprotein, abundantly expressed on neurons, where it was shown that 90% of PrP^C recycle every few minutes between the plasma membrane and early endosomes, after possibly leaving lipid rafts and being endocytosed via clathrin coated pits (Sunyach, Jen et al. 2003). Within this recycling mechanism, PrP^C can be found mainly intracellularly, bound to endocytic vesicles (Ford, Burton et al. 2002). As PrP^C is a GPI-anchored protein, lacking any cytoplasmic domain, it has to bind to transmembrane receptors extracellularly to be endocytosed. It has been shown that the neuronal low-density lipoprotein receptor-related protein1 (LRP1) and the laminin receptor (LRP/LR) act as such receptors for PrP^C and PrP^{Sc} (Parkyn, Vermeulen et al. 2008; Jen, Parkyn et al. 2010). Still it is not known how PrP^{Sc} is internalized, but it has been postulated that PrP^{Sc} might be directly translocated via transporter complexes or by direct penetration of the plasma membrane (Wender, Mitchell et al. 2000; Aguzzi and Rajendran 2009). Besides intracellular trafficking of PrP^C and PrP^{Sc}, intercellular transfer of PrP^C between tissues might be involved in accomplishing its physiological function, whereas the transport of PrP^{Sc} is required for disease progression. Both conformers can be transported by shedding, along axonal transport and tunnelling-nanotubes, but also in a highly efficient manner via viral particles and exosomes (Glatzel and Aguzzi 2000; Ford, Burton et al. 2002; Fevrier and Raposo 2004; Magalhaes, Baron et al. 2005; Porto-Carreiro, Fevrier et al. 2005; Leblanc, Alais et al. 2006; Alais, Simoes et al. 2008; Vella and Hill 2008; Wadia, Schaller et al. 2008; Gousset, Schiff et al. 2009).

2.6 Exosomes

For eukaryotic cells it is important to communicate with surrounding cells and even different and distant tissues. This can be managed via the uptake of nutrients, receiving signals such as cytokines or chemokines, and via the secretion and uptake of proteins or lipids. Therefore cells endocytose macromolecules from the exterior environment or release them into the extracellular space via exocytosis. One way of exocytosis is the fusion of multivesicular bodies (MVBs) or multivesicular endosomes

(MVEs) with the plasma membrane to release their cargo. MVBs are built in various cell types and represent precursors of lytic granules in T lymphocytes, major histocompatibility complex class II (MHC-II)-compartments in antigen-presenting cells, malanosomes in melanocytes, and late MVBs (late MVEs) in most nucleated cells (Blott and Griffiths 2002; Stoorvogel, Kleijmeer et al. 2002; Thery, Zitvogel et al. 2002). These MVBs originate from endocytic vesicles, which are formed by clathrin-dependent or clathrin-independent endocytosis and fuse with early endosomes (Fig. 3.4). Rab-proteins mediate endosomal maturation by orchestrating luminal acidification, changes in protein content, and cellular localisation. When the limiting membrane of late endosomes buds into their lumen, internal luminal vesicles (ILVs) are built within one vesicle (MVB) (Stoorvogel, Strous et al. 1991). ILVs will be delivered to lysosomes for degradation, or alternatively released into the intercellular space, as exosomes, by direct fusion of MVBs to the plasma membrane (Gruenberg and Stenmark 2004; Piper and Katzmann 2007).

Figure 2.4: Formation of MVEs
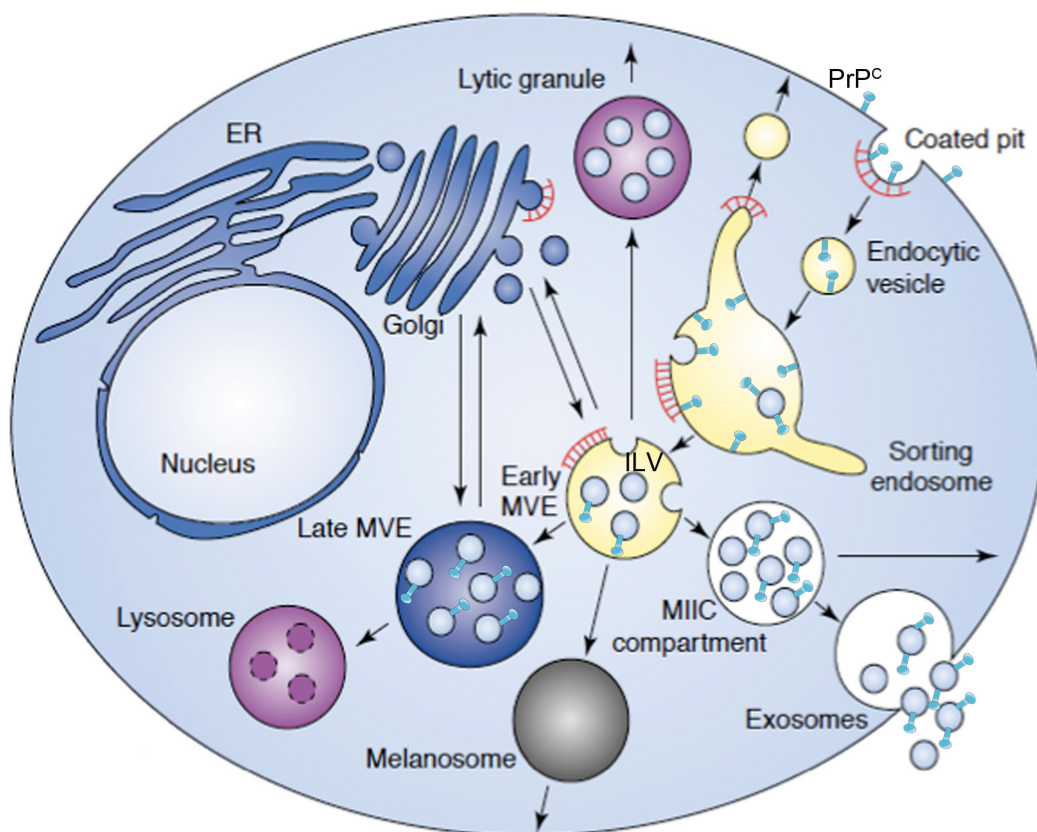Upon invagination of the limiting membrane of sorting endosomes multivesicular endosomes (MVEs) (= multivesicular bodies (MVBs)) are formed. They can represent precursors for lytic granules in T lymphocytes, for melanosomes in melanocytes, MHC-II compartments and exosomes in antigen-presenting cells, and late MVEs (late MVBs) and exosomes in most nucleated cells. Biosynthetic and

endocytic proteins are sorted in an out of MVEs (arrows). Clathrin coats (indicated in red) are found at the trans-golgi network (TGN), on tubular regions of sorting endosomes, and at the plasma membrane. PrP^C (indicated in light green) is found at the plasma membrane, in early endosomes and MVEs. It is transported to lysosomes for degradation or released upon fusion of the limiting MVE membrane with the plasma membrane in exosomes (exocytosed intraluminal vesicles (ILVs)).
(Figure modified after Raiborg *et al.* (Raiborg, Rusten et al. 2003))

Exosomes are small (~100 nm), lipid-raft-rich vesicles released by a variety of cell types including reticulocytes, antigen presenting cells, neoplastic cells, and neurons (Faure, Lachenal et al. 2006; Kramer-Albers, Bretz et al. 2007; Skog, Wurdinger et al. 2008). They are important in antigen presentation, transfer of pathogens, the removal of proteins, and cell communication via the transport of small RNAs (Abusamra, Zhong et al. 2005; Hood, Pan et al. 2009; Simons and Raposo 2009; Silverman, Clos et al. 2010; Testa, Apcher et al. 2010; Zomer, Vendrig et al. 2010; Fitzner, Schnaars et al. 2011; Kogure, Lin et al. 2011); (Gastpar, Gehrmann et al. 2005). By identifying exosomes *in vivo*, in association with follicular dendritic cells (FDCs), malignant tumor effusion, and in urine, their physiological relevance was identified (Denzer, van Eijk et al. 2000; Andre, Schartz et al. 2002; Pisitkun, Shen et al. 2004). They appear to have a function in several different biological pathways dependent on the cell type they are derived from. DC derived exosomes can produce anti-inflammatory response reducing autoimmune diseases and arthritis in mouse models (Kim, Lechman et al. 2005; Kim, Bianco et al. 2006). Interestingly, some proteins, such as the A-Disintegrin-And-Metalloproteinase 10 (ADAM10) are proteolytic active within exosomes and perform proteolytic shedding of target proteins (L1adhesion molecule and CD44) (Stoeck, Keller et al. 2006).

2.7 Internalization of Exosomes

Due to their small size, it is difficult to visualize exosomes and follow their way of internalization by a recipient cell, so most knowledge is based on indirect evidence and electron microscopy. Exosomal protein contents differ a lot depending on their donor cell, but in general they contain endosomal proteins like Alix and Tsg101 acting in the Endosomal Sorting Complex Required for Transport (ESCRT) I-III (Piper and Luzio 2001), distinguishing exosomes from apoptotic blebs and microvesicles (Thery, Boussac et al. 2001), but also lipid raft markers like flotillin and phosphatidylserine, and adhesion molecules, such as the intercellular adhesion molecule 1 (ICAM-1) or tetraspanins involved in the uptake of exosomes by receptor

mediated endocytosis (Wubbolts, Leckie et al. 2003; Morelli, Larregina et al. 2004; Nolte-'t Hoen, Buschow et al. 2009). Furthermore it has been shown that phagocytosis and macropinocytosis are involved in exosomal internalization (Calzolari, Raggi et al. 2006; Feng, Zhao et al. 2010; Fitzner, Schnaars et al. 2011), as well as clathrin-dependent endocytosis followed by fusion of exosomes with the limiting membrane of endosomes (Thery, Zitvogel et al. 2002). In contrast to the internalization of whole vesicles into endocytic compartments, direct fusion of exosomes with the plasma membrane may occur, releasing the exosomal content into the cytosol of the recipient cell (Parolini, Federici et al. 2009; Thery, Ostrowski et al. 2009).

2.8 The Prion Protein and Exosomes

An emerging role for exosomes in neurodegenerative diseases such as Alzheimer`s disease (AD) and prion diseases has been shown as PrP^C and the amyloid precursor protein (APP) are enriched within exosomes (Vella, Sharples et al. 2008) released by various cell types, such as macrophages and neurons (Wang, Zhou et al. 2010). First, endogenous PrP^C was found to be enriched on exosomes released by cells of the male reproductive tract (Ecroyd, Sarradin et al. 2004; Sullivan, Saez et al. 2005), on activated platelet-derived exosomes (isolated from human blood samples) (Robertson, Booth et al. 2006), and on ovine cerebral spinal fluid (CSF) derived exosomes (Vella, Greenwood et al. 2008). Considering the way of PrP^{Sc} spreads within an organism, exosomes were thought to provide an excellent vector for the infectivity. This idea was confirmed using murine neuroglial cell lines overexpressing ovine PrP (Fevrier, Vilette et al. 2004; Porto-Carreiro, Fevrier et al. 2005). Even prion infectivity could be spread to recipient cells via PrP^{Sc}-containing exosomes, especially if cells (fibroblasts) were co-transfected with retroviral particles, which enhance the release of exosomes and hence the transmission on PrP^{Sc} (Leblanc, Alais et al. 2006). Apart from this disease-conveying role in case of PrP^{Sc} formation, it seems that PrP^C is not randomly found in exosomes, but rather specifically released via exosomes depending on the donor cell. For instance, some cell types, like thyroid cells, release soluble PrP^C into the medium but not associated with exosomes (Campana, Caputo et al. 2007). Cell-specific internalization of PrP^C into exosomes suggests a particular function of PrP^C in intercellular signalling (Liu, Li et al. 2002). As PrP^C is GPI-anchored, it might be sequestered to exosomes because of

its association within lipid rafts, making it more prone to be packaged into ILVs (de Gassart, Geminard et al. 2003). Sorting of proteins into MVBs is thought to involve, but not require ubiquitination of proteins (Reggiori and Pelham 2001; Raiborg, Rusten et al. 2003; Babst 2005). Though this process is very complex, it seems that especially the diglycosylated form of PrP^C is sorted into exosome and possibly N-terminal modified (Vella, Sharples et al. 2007) pointing to a highly specific sorting of PrP^C to MVBs.

3. Objective of the Thesis

The release of PrP^C and PrP^{Sc} via neuronal exosomes has been shown in previous studies. Exosomes could transport PrP^{Sc} intercellularly and therefore promote infectivity. One aim of this thesis was to examine the intercellular trafficking of neuron-derived exosomes in the absence of PrP^C. Exosomal internalization is not completely understood, but receptor mediated endocytosis has been shown to be one pathway in some cell types. As PrP^C interacts with several membrane proteins, it might be involved in the internalization process of exosomes. The possible function of PrP^C in exosomal transport, specifically in exosomal uptake should be addressed in this thesis using primary neurons and neuronal cell lines containing or lacking PrP^C. To achieve reliable results, a quantitative uptake assay should be established in this study allowing the determination of PrP^C dependent exosomal uptake efficiencies by recipient neuronal cells. Furthermore the intracellular pathway of exosomes should be examined and checked for a possible PrP^C dependence. Finally, we want to verify how the findings gained in this study fit with previously suggested physiological functions of PrP^C.

The results gained in this study will provide better insight into exosomal trafficking in neurons and reveal a novel physiological function for PrP^C.

4 MATERIAL

4.1 Equipment

Product	company, country
6 cm Plastic dishes	Sarstedt, Germany
8-channel pipette 100-1000µl	Eppendorf, Germany
8-channel pipette 10-100µl	Eppendorf, Germany
8-channel pipette 1-10µl	Eppendorf, Germany
15-ml Reaction Tube	Greiner Bio-One, Germany
50-ml Reaction Tube	Greiner Bio-One, Germany
1,5 ml Reaction Tube	Eppendorf (Hamburg)
2 ml Reaction Tube	Eppendorf (Hamburg)
Autoclave	Memmert, Germany
Bacteria incubator	Heraeus electronics, Germany
Balance Shinko Denshi	Vibra, Japan
Balance precision MC1 polyorange RC 210 P	Sartorius, Germany
Cell culture dish, 6 wells, sterile	Nunc, Germany
Centrifuge 5415 R, refrigerated, rotor F45-24-11	Eppendorf, Hamburg
Centrifuge, mini MC 6	Sarstedt, German
Cover slip	Assistant, Germany
Electron microscope CM12	Philips, Germany
Electrophoreses, mini	BioRad, Germany
FACSCalibur	Becton Dickinson, UK
FACS Cantoll	Cantoll, Germany
FlowJo Software	Tree Star, USA
Fluoromount G	SouthernBiotech, USA
Filter-Tube (0,22 µm)	Millipore (Massachusetts, USA)
Gel caster & comb	BioRad, Germany
Gel documentation DeVision G	Decon Science Tec GmbH, Germany
Hypercassette^{TM}	GE Heakthcare, UK
ICycler Thermal Cycler	BioRad, Germany

ImageJ software	NIH, USA
Imaging system Chemi Doc^{TM}	BioRad, Germany
Incubator (cell culture)	Heraeus, Germany
Incubator (immunohistochemy)	Memmert, Germany
Lser scanning confocal microscope TCS Sp2	Leica, Germany
Ultraview Vox 3D Imaging System	Perkin Elmer, USA
MyCycler Thermal cycler (PCR)	BioRad, Germany
Neubauer counting chamber	Assistant, Germany
Paper cutting machine	Roth, Germany
PH meter CG 840	Shott, Germany
Photometer, biophotometer plus	Eppendorf, Germany
Pipette boy	Integra Bioscience, Germany
Pipette research fix 0,1-2,5 µl	Eppendorf, Germany
Pipette research fix 100-1000 µl	Eppendorf, Germany
Pipette research fix 10-100 µl	Eppendorf, Germany
Pipette research fix 1-10 µl	Eppendorf, Germany
Powersupply easy volt	Stratagene, Germany
Powersupply, PowerPac basic	BioRad, Germany
Printer P93D	Mitsubishi, Germany
PVDf membranes	BioRad, Germany
Spectrosize 300 sls/dls spectrometer	Molecular Dimensions, UK
Ultracentrifuge L-60, rotor SW40-Ti	Beckman Coulter, USA
Vortex genie 2	Scientific industries, USA
Waterbath	P-D Industriegesellschaft, Germany

4.2 Cell lines

Table 4.1: Cell lines used in this thesis. Listed are the cell lines used, each with the correct cell name, the cell type including its characteristics, and the source

Cell Name	Cell Type	Source
N2a 299	Neuroblastoma, mouse	AG Glatzel, UKE, Germany
HpL-3,4	Hippocampus, Prion knockout mouse	T. Onodera, Ibaraki, Japan
PrP^{3F4}	Stabile transfected with 3F4 mAb epitope tagged PrnpcDNA HpL3,4	UKE, Germany in collaboration with Dr. S. Krasemann & P. Lüpke
NiH 3T3	Fibroblasts, mouse	AG Kutsche, UKE, Germany

4.3 Chemicals and Detergents

All chemicals and detergents used in this study were listed in an alphabetical order. If not stated otherwise, salts, acids and bases were from Merck, Darmstadt, Sigma-Aldrich, Munich or Fluka, Neu Ulm

Product	company, country
Acetic acid	Roth, Germany
Acrylamide/Bisacrylamide	Roth, Germany
Agarose	Invitrogen, Germany
AlexaFluor594-labeled holotransferrin	Invitrogen, Germany
Ammoniumpersulfat (APS)	Roth, Germany
Autoclaved aqua bidest.	UKE, Germany
Bromphenol blue	Merck, Germany
Ethanol	UKE, Germany
Cytosin arabinoside (AraC)	Sigma-Adrich (Taufkirchen)
Developing machine western blot	AGFA, Germany
Donkey serum for IF	Dianova, Germany
ECL western blotting substrate	Thermo Scientific, Germany

Ethylenediaminetetraaceticacid (EDTA)	Sigma, Germany
Dimethyl sulfoxide (DMSO)	Sigma, Germany
G418 (Gentamycin) supliate solution (50 mg/ml)	PAA, Austria
Hoechst342	Invitrogen, Germany
LysoTracker red	Invitrogen, Germany
Methanol	J.T. Baker, Germany
N,N,N`,N`-Tetramethylethylendiamine (TEMED)	Sigma, Germany
Page Ruler^{TM}, Prestained Protein Ladder	Fermentas, Germany
Ponceau S	Sigma, Germany
Poly-L-Lysin	Sigma-Aldrich, Germany
Potassium chloride	Fluka, Germany
Potassium dihydrogen phosphate (KH_2PO_4)	Merck, Germany
Sodiumdodecylsulfate (SDS)	Sigma, Germany
SuperSignal West Femto	Thermo Scientific, Germany
SuperSignal West Pico	Thermo Scientific, Germany
Tris(hydroxymethyl).aminomethan (Tris)	Sigma, Germany
Tween 20 (polyethylene-sorbitane monolaurate)	Roth, Germany

4.4 Kits, Enzymes, Nucleotides, and Standards

Fugene6	Roche Biochemials, Germany
(Fluorescent) Cell Linker Dyes	Sigma-Aldrich, Germany
Lipofectamine 2000	Invitrogen, Germany

4.5 Antibodies

Table 4.2: Primary antibodies
All primary antibodies are listed with their application and the best working dilution.

Antibody	Dilution	Application	Source
AIP-1	1:1000	WB	BDPharmingen,Germany
Tsg101	1:1000	WB	BDPharmingen,Germany
GM130	1:300	WB	BDPharmingen,Germany
LBPA	1:25	IF	J. Gruenberg,Austria
Rab4	1.100	IF	BDPharmingen,Germany
Flotillin-1	1:1000	WB	BDPharmingen,Germany
PomII	1:1000	WB	A. Aguzzi, Switzerland
3F4	1:1000	WB	Covance, USA

Table 4.3: Secondary antibodies
All secondary antibodies are listed with the dilution used and their application

Antibody	Dilution	Application	Source
Goat anti-mouse IgG, HRP	1:2000	WB	Promega, Germany
Goat anti-mouse Alexa555	1:250	WB	Invitrogen, Germany

4.6 Media and Supplements for Cell Culture work

Dulbecco`s Modified Eagle Medium, high glucose (DMEM)	PAA Laboratories (Paschingen, Austria)
Minimal Essential Medium (MEM)	Invitrogen Germany
Neurobasal Medium	Invitrogen Germany
Opti-MEM ®	Invitrogen, Germany
Hank`s Buffered Salt Solution (HBSS) 10x	Invitrogen, Germany
Fetal Calf Serum (FCS)	Gibco Invitrogen, Germany
Horse Serum (HS)	Gibco Invitrogen, Germany
L-Glutamine, 200 mM	Sigma-Aldrich, Germany
Penicillin/Streptomycin Solution	PAA Laboratories, Austria
B 27 Supplement	Gibco Invitrogen, Germany
Phosphate Buffer Saline (PBS)	Gibco Invitrogen, Germany

4.7 Buffers and solutions

Electrophoresis Buffer (10x)

30 g/l Tris

144 g/l Glycin

10 g/l SDS

Wetblot-Buffer (10x)

30,3 g Tris

144 g/l Glycine

PBS (10x)

80   g/l NaCl

 2   g/l KCl

11,5 g/l Disodium hydrogen phosphate (Na_2HPO_4)

2   g/l Potassium dihydrogen phosphate (K_2HPO4)

pH = 6,9 (10x), 7,3 (1x)

TBST (10x)

12,11 g/l (100 mM) Tris

81,81 g/l (1,4 mM) NaCl

pH = 7,4; + 1 % Tween + add H_2O up to 1 litre final volume

.

TAE (50x)

242 g Tris-Base

57,1 ml acetic acid

100 ml 0,5M EDTA, pH 8,0 + add H_2O up to 1 litre final volume

Half synthetic glycerine medium (HSG)

13,5 g/l Casein/Peptone

12,5 g/l NaCl

 7,0 g/l Yeast extract

17   g/l 87% Glycerine

2,3 g/l K_2HPO_4

1,5 g/l $MgSO_4$ + add H_2O up to 1 litre final volume

pH= 7,4

Paraformaldehyde solutions

2-4 g Paraformaldehyde (for 2-4%)

80 ml dH_2O

50 µl 5M NaOH

→ Heating to 50°C, work under flow! + 10 ml PBS (10x) + H_2O/ 100 ml

→ pH = 7,4; aliquot and freeze at – 20°C.

HBSS:

10 ml HBSS 10x

1 ml HEPES 1M

500 µl $NaHCO_3$ 7,5%

+ P/S 1:100 + add H_2O up to 100 ml final volume

→ Sterile filtration!

MEM-HS:

10 ml HS

 3 ml $NaHCO_3$ 7,5%

 6 ml Glucose 10%

81 ml MEM 1x

+ P/S 1:100 + add H_2O up to 100 ml final volume

→ Sterile filtration!

Neurobasal Medium:

100 ml Neurobasal Medium

2 ml B27 Supplement

250 µl glutamine

+ P/S 1:100

→ Sterile filtration!

5 METHODS

5.1 Cell Culture

5.1.1 Cultivating Cell lines

Adherent cell lines (N2a, HpL3-4, PrP^{3F4}) were cultured in T75 culture flasks (surface = 75 π cm^2) at 37°C, 5%CO$_2$ in DMEM (high glucose= 4,5 g/l); 500 ml DMEM high glucose (+ 5 ml P/S, 50 ml FCS (= 10%)).

Every fresh prepared medium was checked for sterility by incubating a small aliquot for few days in the cell culture incubator. Cell culture work was performed at sterile conditions, working under a clean bench. For different experimental approaches, cells were seeded on T75-flasks, 6 π cm^2 plastic dishes, 6 π cm^2 glass bottom dishes, or coverslips (4 coverslips/ well in a 6-well-plate). For immunofluorescence staining, cells were grown to the pint of 80% confluence.

5.1.2 Splitting Cells

Cells were split as often as needed depending on he experiments, but usually every second day at a confluence ranging from 80-100%. For passaging, medium was taken off, cells were carefully washed in 10 ml PBS, PBS was drawn off, the cells were incubated in 1 ml trypsin (if necessary at 37°C) until all cells detached from the bottom. Then 5 ml DMEM was added to stop the trypsination reaction. Depending on the desired confluence half of the medium (up to a 6th of the medium) remained in the flask and the adequate amount of DMEM was added to yield an end volume of 20 ml DMEM /75-flask.

5.1.3 Freezing Cells

The cell lines could be stored for several months, when kept at -80°C in special freezing medium (= 50 % DMEM (high glucose) + 10% DMSO + 40% FBS) containing DMSO to prevent the formation of ice crystals. The cells were split 1/3 as described above, then the cells in solution were spun down 5 min at 300xg, the supernatant was discarded and the 1/3-pellet was resuspended in 1 ml ice cold freezing medium. The solution was filled into a criovar, which was immediately kept cool, by transferring it into an isopropanol filled freezing box. This box was then stored at -80°C overnight and then the criovars containing frozen cells were put into paperback boxes and stocked at -80°C.

5.1.4 Revitalizing Cells

For revitalization, frozen cells (1 – 1,5 ml) were taken out of -80°C freezer and the cells started thawing due to body heat of the hands. They were put into warm DMEM (18,5 – 19 ml) and cultured in a T75-flask over night. The next morning the cells were attached to the bottom of the flask and the medium was exchanged for DMSO-free DMEM.

5.1.5 Cell Transfection

Foreign DNA can be inserted via a plasmid into eukaryotic cells either transiently or stably (via recombination into the genome) via transfection. In this study cells were in general transfected via lipofection using Lipofectamine2000. One day before transfection, cells were split (1-2 x 10^4 cells/cm^2) in medium without antibiotic on 6-Well-Plates to achieve a 50 to 70 % confluence of vital cells at the day of transfection. To ensure that the expression of the reporter gene is not due to insertion of non complex DNA and that the activity measured is not only background, three wells which function as negative controls (cells+ "naked" DNA, cells+ non-coding DNA+ transfection reagent, and no DNA + no transfection reagent) should be carried along with the transfection process. Two different Lipofectamine solutions were prepared: a) 8 µl Lipofectamine + 242 µl Opti-Mem (=1:2 dilution), b) 16 µl Lipofectamine + 234 µl Opti-Mem (1:4 dilution) and 4 µg DNA were carefully mixed in 250 µl Opti-Mem, twice. Then 250 µl of the Lipofectamine solution a) and b) were directly transferred to 250 µl DNA solution (without touching the wall of the tube), mixed carefully and incubated at RT for 20 minutes to allow DNA-lipid-complexes to build, before the mixture is transferred to the cells (500 µl DNA-Lipofectamine-Mix / well) in 1,5 ml Opti-Mem without antibiotics. During a 4 - 6 h incubation step at 37°C, 5% CO_2, the DNA-lipid-complexes can be taken up by the cells. Then the medium is exchanged against fresh medium containing the selective antibiotic, which is lethal for cells without the specific antibiotic resistance encoded in the transfected plasmid, causing selective growth of only successfully transfected cells.

5.1.6 Generating a stably transfected cell line

The neuronal PrP^C knockout cell line (PrP$^{-/-}$) was transfected with a mouse 3F4-tagged PrP-construct (in expression vector pCDNA3.1-Zeo). On the following day,

cells were split strongly (1:20-1:40) to provoke their separated growth. To select for cells successfully transfected, Zeocin (antibiotic) was added to the medium (1mg/ml), which is lethal to the cells without Zeocin-resistance. The cells were allowed to grow for 7 days at 37°C, 5% CO_2. Next, depending on their confluency, cells were split again for greater separation. On day 10 after transfection single cell clones were picked using a microscope (extensively cleaned previously) in the cell culture flow bench and a cloning ring. The clones were grown on different dishes for single clone colonies. The amount of PrP^{3F4}-expression of those colonies was detected via western blot. Cell cultures with very low expression of PrP^{3F4} were discarded, whereas cell cultures with a high expression rate were kept in culture and several samples were stored at -80°C for future use.

5.1.7 Preparation of primary neurons

Primary neurons were obtained from PrP^C knockout ($PrP^{-/-}$) (Büeler, 1992) and PrP^C containing (wt; C57BL/6) mice, embryonic day 14,5 (E 14,5). First HBSS was put in water bath at 37°C and a 10 cm bacterial dish (for uterus), a 10 ml HBSS in 15-ml falcon tube, and 1/10 trypsin in HBSS (500µl HBSS+ trypsin/embryo) were prepared. To start with preparation, skin of a pregnant mouse was opened, uterus was taken out and put into bacterial dish (HBSS); embryos were separated from uterus and yolk sac and every embryo was put into a separate small dish (HBSS). The embryonic head was cut off, fixed with tweezers (in the eyes), skull was opened with a small scissor by cutting along the midline, starting at the back of the head going towards the eyes and pulling open the skull. Brain was peeled out with tweezers and meninges and medulla oblongata were removed. After cutting the brain into small pieces, they were transferred to 10 ml HBSS in falcon tube (at least 1ml HBSS/embryo, maximum 4 embryos/10 ml HBSS). This medium was exchanged against 500 µl 0,25 % trypsin in HBSS/embryo and incubated for 15 min (gently shake in between) at 37 °C (After trypsination: No use of vacuum pump!). Cells were washed three times in 1ml/5ml HBSS, the final volume HBSS (600 µl/embryo) was put and the cells were dissociated in HBSS using Pasteur Pipets (fire-polished big opening to smaller) by pipetting up and down. Dissociated cells were plated onto PLL-coated dishes with MEM-HS: 300 µl/dish and after 4 hours the medium was replaced by Neurobasal Medium (pre incubated at 37 °C, 5 %CO_2, 30 min). The day after, 1 mM AraC (5 µM) was added to neurons (990 µl H_2O+ 10 µl AraC (0,1M

stock)) diluted 1/200 in Neurobasal Medium (= 15 µl AraC/ 3 ml Neurobasal). After 4four hours of incubation at 37 °C, 5 % CO_2, MEM-HS Medium was exchanged against Neurobasal Medium.

5.2 Exosomal methods

5.2.1 Harvesting exosomes

To harvest exosomes from cell lines or primary neurons, the supernatant (Opti-MEM for cell lines and Neurobasal Medium for primary neurons) was taken and transferred into a falcon tube. The exosomal pellet was obtained by serial centrifugation of these supernatants as the cells released exosomes into the medium. First, the supernatants were spun down for six min at 300 x g to get rid of dead cells, then the supernatant was transferred into a fresh falcon tube and spin down again for additional 30 min at 5000xg to pellet cell debris, additional 30 min at 20000xg to get pellet big vesicles and membranes, then the supernatants were purified and concentrated down to 1,5 ml through a 0,22 µm filter-tube. The final centrifugation at 120000xg for 1 hour revealed the pure exosomal pellet.

5.2.2 Labelling exosomes

To follow the route of the exosomes with confocal microscopy or Flow-cytometry analysis, they were fluorescently labelled using a lipophilic PKH fluorescent cell linker dye, staining the membrane of the exosomes. With the help of this dye, exosomes could be either labelled via a green PKH67 (excitation = 490 nm; emission = 504 nm) or a red PKH26 (excitation = 551nm; emission = 567 nm) fluorochrome. The pure exosomal pellet was resuspended in 100 µl PBS (+PI), 900 µl Dilution C (included in kit) and 1 µl fluorescent dye (PKH26/PKH67) were added. To mix the components, sample was vortexed and then incubated 5 min RT (dark). Next, 200 µl FCS were added and the solution was vortexed to stop the reaction. With another 1 hour centrifugation at 100.000 x g, 4°C, fluorescent-labelled exosomes were pelleted and the supernatant was taken off.

5.2.3 Light Scattering Techniques

In this study, it is essential to quantify and compare the amount of exosomes in the different samples. The quantification of exosomes was achieved using Static and Dynamic Light Scattering (SLS/DLS) with SpectroSize3000. In Light Scattering

Techniques a laser (660 nm) strikes particles in solution, an oscillating electric field is build, the particles polarise and move due to Brownian motion according to their size scattering light in every direction. The scattered photons are detected by a photon detector, which is oriented to the solution in a 90° angle (Fig. 4.1).
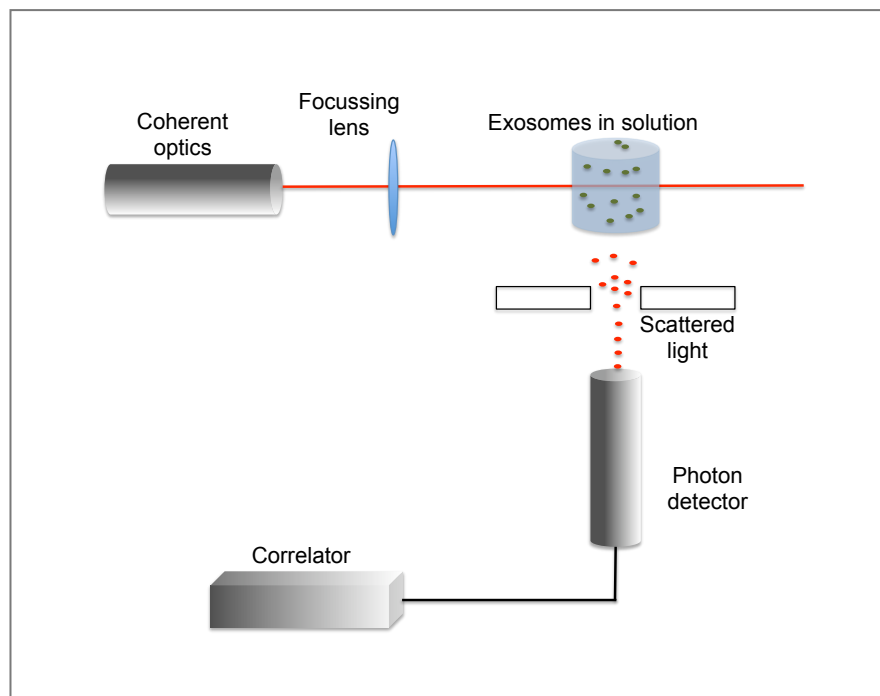

Fig. 5.1: Schematic diagram of a conventional 90° Light Scattering instrument.
The laser strikes the particles in solution, light will be scattered by the particles, transferred to the photon detector, and converted to electrical pulses. The correlator generates the autocorrelation function out of these electrical pulses.

The intensity fluctuations of that light are converted into electrical pulses, which are transferred to a correlator to generate the autocorrelate function, which is needed to carry out the actual data analysis. In DLS the dynamics of the scattered light are determined and analysed. In our set up, the most intense signal scattered by the solution was standardised to 1 and the relative proportion of particles was measured, producing a mean radius distribution. The time average intensity of scattered light (SLS) was captured during the same measurement resulting in a certain count rate (kHz).

5.2.4 Electron microscopy

To analyse exosomes with electron microscopy, the vesicles had to be fixed on a copper grid. Previous to the fixation, the pure exosomal pellet containing approximately 2×10^8 exosomes/ml, was resuspended in 10 µl PBS (+PI), then 20 µl 2% Paraformaldehyde was added, the solution was incubated for 30 minutes at 4°C

and 5 µl of the exosome-solution was transferred to a 600-mesh carbon-coated copper grid and incubated in a wet chamber for 20 minutes at RT. Following three washes with PBS, the exosomes were fixed on the grid with 1% Glutaraldehyde, the grid was dried with a paper tissue and the exosomes were incubated for 10 minutes in saturated lead for contrasting the sample. As a second option, the exosomes were placed on the copper grid, incubated for 90 seconds, washed twice with H_2O for 10 seconds, and were then negatively stained with uranyl acetate for 60 seconds. After complete drying, the specimens were examined with a Philips CM12 electron microscope 100 kV by Dr. Lars Redecke.

5.2.5 Sucrose density gradient

To analyse the specific density of the purified vesicles, a sucrose density gradient was created with a range from 1,07 - 1,5 g/cm^3 sucrose (in HEPES) in an ultracentrifuge tube (total volume of 13 ml). The purified exosomes were resuspended in 25 µl PBS and transferred to the sucrose gradient. After 16h of centrifugation at 100.000 x g (4°C) the different fractions (representing different sucrose concentrations) were recovered from the sucrose density gradient, concentrations were calculated using a refract meter, and the fractions were loaded onto a SDS-PAGE before protein contents were detected using western blot analysis.

5.2.6 SDS-Polyacrylamid gel electrophoresis (SDS-PAGE)

To separate proteins within one sample, discontinuous gel electrophoreses were performed using polyacrylamide as carrier, based on its strong resolution power. In principle electrophoreses separate proteins due to their characteristic migration within an electric field in which they have to pass the three-dimensional network built by polyacrylamide. The pore size of this network can be altered depending on the concentration of acrylamide within the gel and it is adjusted depending on the size range of proteins that should be separated. Usually the lower part of the gel was higher concentrated in acrylamide (12%) to especially separate the proteins ranging from16 to 60 kDa (including PrP^C). In the upper and less concentrated (4%) part of the gel, pores are wider and the proteins were gathered and stacked according to their motility within the electric field, gaining a pre separation and accumulation of proteins at the border towards the separation gel. These discontinuous gels were

cast between two absolutely clean glass plates, stabilised by a special holder. First the 12% separation gel was prepared according to the recipe below and after polymerisation the 4% collection gel was added on top and a plastic comb was put into the gel to build the sample pockets within the acrylamide during the polymerisation. 10% APS and TEMED were added last, because they will start the polymerisation process. The polymerised gels were transferred into a tank filled with electrophoresis buffer (1x) and the samples were prepared.

Previous to a gel electrophoresis, loading dye (10x CLV) was added to the protein sample (under the air flow), the enclosed β-mercaptoethanol could break the disulphide bonds in the polypeptide chains, and then the proteins were denatured by heating the sample (including loading dye) for 10 minutes at 96°C (sample can be stored at -20°C).

Table 5.1: Composition of a SDS-PAGE
All components of a SDS-PAGE and their amounts are listed.

Reagent	12 %	4%
H_2O	5,05 ml	3ml
1,5 M TrisHCl pH8, 8	2,6 ml	----
30% BisAcrylamid	4,2 ml	0,65 ml
10% SDS	0,525 ml	250 µl
10% APS	70 µl	100 µl
TEMED	7 µl	10 µl
0,5 M TrisHCl pH 6,8	---	1,25 ml

The samples were loaded into the pockets of the gel, 4 µl of a protein marker were loaded as well and the voltage was set to 80 mV until the samples reached the border to the separation gel. Then the voltage was increased to 100 mV until the marker was nicely separated within the gel. The proteins were separated and the gel was transferred into a small box filled with wet-blot-buffer (1x).

5.2.7 Western blot

In the Western blot procedure the separated proteins will be transferred from the gel to a protein binding membrane, in an energised process, where they can be immunochemically detected afterwards. For Immuno-Blotting, the wet-blot-system

was used, allowing the blotting of two gels in parallel for a wide range of protein sizes. Before use, the x10 wet-blot-buffer had to be diluted: 100 ml buffer, for detection of proteins $\geq$ 30 kDa add 10 % methanol, for proteins $\leq$ 30 kDa add 20 % methanol, filled up with aqua dest. to 1 litre final volume. Per gel to blot, 2 thin plastic sponges and 4 Whatman papers were shortly incubated in wet-blot-buffer and one Polyvinylidendifluorid (PVDf) membrane was activated with pure methanol and then washed in wet-blot-buffer. Proteins are blotted from cathode (-) to anode (+), so the layers will be built as following: cathode (black), sponge, 2x Whatman paper, gel, membrane, and 2x Whatman paper, sponge. The proteins were blotted to the PVDf membrane in a BioRad wet-blot tank for one hour at constant 200 mA/membrane.

After blotting, the gel was discarded and the membrane was blocked in 5% milk in TBST for 30 minutes up to an hour, RT. Antibodies were added at the indicated dilution (tableNO) in 5 % milk in TBST O/N at 4 °C. Next day, the first antibody was taken off and the membrane was washed with 5 % milk in TBST for 10 minutes, then washed twice with TBST only (for 5 minutes), then the secondary antibody in 5 % milk-TBST was added in the indicated dilution and incubated on the membrane for one hour, RT, shaking. After discarding the secondary antibody, the membrane was washed 3 times for five minutes in TBST, RT.

Detection of the proteins was performed using PICO and visualisation by Quantity One 4.6.2 Software (BioRad).

5.3. Exosomal Uptake Assay

To analyse the different quality of exosomal uptake depending on the abundance of PrP^C on the membrane, exosomes were co incubated with recipient cells and the amount of exosomes taken up was determined. The recipient cells were either grown on glass coverslips or glass bottom petri dishes to 80% confluence of vital cells. Pure exosomal pellets released by neuronal CL or PN were labelled with PKH26 or PKH67 as described above and spun down at 100.000 x g for one h to gain pure pellets of fluorescent labelled exosomes. These pellets were resuspended in warm cell culture medium and exosomes were incubated with recipient cells for a specific time point (depending on the question addressed) at 37°C, 5% CO_2. Endocytosis was stopped by the transfer of cell cultures to 4°C and a cold PBS wash, stripping non-internalized exosomes.

5.4 LysoTracker Uptake

To follow late endosomal and lysosomal sorting of exosomes, recipient neuronal cells were grown on glass coverslips to 80% confluence. The recipient cells were incubated with 75 nM LysoTracker red (in pre-warmed DMEM) for 30 min at 37 °C, 5% CO_2 to be internalized by recipient cells and stain acidic compartments fluorescently red. In the last 20 min of incubation 20 µg/ml Hoechst342 were added. Hoechst will label DNA in blue fluorescently and the nucleus will be visualized.

Next, the medium will be exchanged and fluorescent-labelled exosomes (stained with PKH67) will be co-incubated with the recipient neuronal cells. After 30 min of incubation at 37 °C, 5 % CO_2 medium was exchanged against exosome-free warm (37 °C) medium and endocytosis of exosomes to acidic compartments was monitored taking z-stacks of the cells with a confocal laser scanner microscope (Perkin Elmer, Ultraview Vox 3D Imaging System) for 35 minute additionally. The amount of exosomes co-locating with LysoTracker was calculated using ImageJ software.

5.5 Transferrin (TfR) Uptake

For the uptake of holotransferrin, cells were grown on glass bottom dishes to a confluence of up to 80 %. Holotransferrin is a glycoprotein that interacts with the type I transferrin receptor (TfR) and gets internalized into acidic compartments. Within the first hour of internalization TfR will recycle to the plasma membrane via Rab4-positive recycling endosomes. To track that recycling process, 5 µg/ml AlexaFluor594-labeled holotransferrin was added to the medium of neuronal cell lines (PrP^C, PrP$^{-/-}$, and PrP^{3F4}). Within one h incubation at 37 °C, 5 % CO_2, AlexaFluor594-labeled holotransferrin was allowed to be endocytosed. Then the medium was taken off, the recipient cells were washed with cold PBS and fixed with 4 % Paraformaldehyde. After drying consecutive z-stacks were taken with the laser scanning confocal microscope (Leica Laser Scanning Confocal Microscope TCS SP2). Next, the fluorescent intensity per cell volume was determined using ImageJ software.

5.6 Flow-Cytometry Analysis

For the analysis of exosomal internalization following co-incubation of recipient cells and fluorescent-labelled exosomes, flow-cytometry was used. After the specific incubation time, cells culture dishes were kept on ice to stop endocytosis, washed 3 times with ice-cold PBS, a final volume of 500 µl PBS was added, and the cells were

released from the bottom of the culture dish carefully using a cell scraper. The samples were kept on ice until they were analysed via flow-cytometry. In a flow cytometer, cells in solution are aligned so that they pass a light beam as single cells. Depending on the exosomal labelling (red or green) a low-power air-cooled laser red-HeNe (633 nm), or green-HeNe was used to provoke light signals in the cell solution. The forward and sideward scattered signals, resulting of light scattered by the cells, were detected and cells could be differentiated from eventual contamination by size exclusion. The cell-specific fluorescence signal was also detected and calculated into electric signals. A computer connected to the flow cytometer using Becton-Dickinson software performed the acquisition.

5.7 Immunofluorescence

To see whether the exosomes co localize with certain compartments of their recipient cells after performing an uptake assay, these compartments were immunofluorescently stained. Therefore the cells were either grown on sterile (autoclaved) glass coverslips or on sterile glass bottom dishes to the point of a confluence of 80 % previously. After finishing the uptake assay, cells were fixed with 4 % Paraformaldehyde for 20 minutes RT, then incubated for 15 minutes in PBS+ 0,1 % Triton-X100, RT, blocked with donkey serum (1,2 nm/ml) diluted 1:50 in PBS for 15 min, RT (≈ 50 µl/Coverslip). After blocking of the unspecific free binding sites, the donkey serum is removed from the cells and a primary antibody diluted (see table 4.2) in 1:50 Donkey serum-PBS is added onto the cells. Primary antibodies derived from different species can be used in parallel. The primary antibody should be incubated for at least 20 minutes and up to O/N. Then the cells were washed with PBS+ 0,1 % Triton-X100 for 15 min, before the secondary antibody was added (see table 4.3) diluted in Donkey serum-PBS and incubated 20 min to 1 h, RT in the dark. Following two washes with PBS, the coverslips were mounted onto a microscope slide or glass bottom dishes where they were sealed with mounting medium Fluoromount G. The mounting medium was dried at 37 °C for three hours or at RT O/N, always kept in the dark and could then be analysed by confocal microscopy.

5.8 Statistical analysis

For statistical comparison of Flow-cytometry or immunofluorescence-based quantifications, Student`s t-test was used with levels for statistical significance set at p-values < 0,05 (*), < 0,01 (**), and < 0,001 (***).

6. RESULTS

6.1 Characterization of exosomes derived from neuronal cell lines and primary neurons

Isolation of pure exosomes is typically achieved by serial centrifugation of cell culture supernatants. Due to their apparent endosomal biogenesis, exosomes have been found enriched in the ESCRT-proteins AIP-1 (ALG-2-Interacting-Protein; or Alix) and Tsg101 (Tumor Susceptibility Gene 101) and in the lipid-raft-protein Flotillin-1, and thus, these proteins are used as exosomal marker proteins. The purity of the exosomal purification and verification of possible contamination from lysis-derived cell organelles can be achieved by testing the presence of the Golgi-Marker-Protein (GM130) in exosome fractions. After harvesting exosomes via serial centrifugation steps, which was shown to effectively separate exosomes from non-exosomal membrane vesicles, membranous fragments, and other contaminants, the pellet was resuspended in 25 µl PBS (+PI), loading buffer was added and the pellet was analyzed via SDS-PAGE and Western blot.
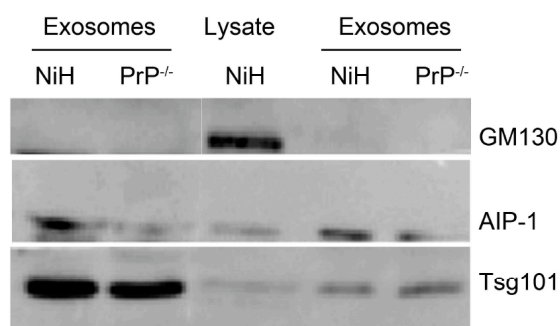

Fig.6.1: Western blot of cell line-derived exosomes
Exosomes were purified from supernatants of a fibroblast cell line (NiH) and the neuronal PrP-knockout cell line (PrP$^{-/-}$) via serial centrifugation and subjected to Western blot analysis following SDS-PAGE. The expression of exosomal markers (AIP-1; Tsg101) within these fractions was shown. The Golgi marker (GM130) was only found in the lysate control. The samples resulting out of serial centrifugation contain pure exosomal fractions released by NiH-CL and PrP$^{-/-}$-CL.

Via Western blot analysis exosomal markers were detected for exosomes released by PrP$^{-/-}$-CL. Exosomal fraction derived from NiH-3T3 fibroblasts served as a positive control for the exosomal purification. We could show that the purification of exosomes worked and that the PrP$^{-/-}$ cell line (PrP$^{-/-}$-CL) releases exosomes in the supernatant (Fig.6.1).

6.1.1 Exosomes derived from neuronal cell lines and primary neurons

To characterize exosomes derived from neuronal cell lines and primary neurons, first exosomes released by the PrP^C containing Neuroblastoma cell line N2a (PrP^C-CL) and exosomes released by wild type primary neurons (PrP^C-PN) in culture, were isolated and subjected to western blot analysis. Typically one sample consisted of ~4-8 x10^8 exosomes. Besides the exosomal marker proteins, the samples were tested for their PrP^C load using the prion-antibody PomII.
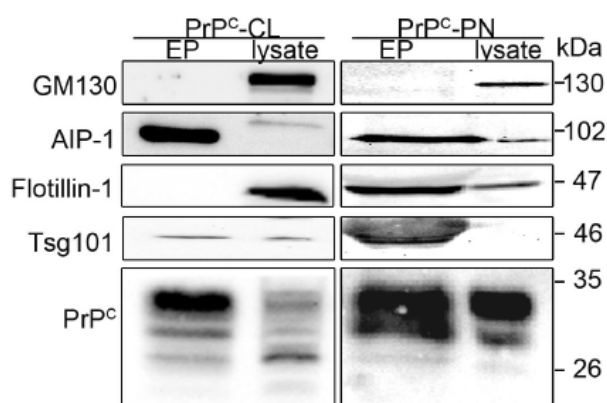

Fig.6.2: Western blot of PrP^C-CL- and PrP^C-PN-exosomes and lysates
Exosomes were purified from supernatants of the neuroblastoma cell line N2a (PrP^C-CL) and primary neurons (PrP^C-PN) (E14) by serial centrifugation. Exosomal pellets (EP) (≈ 4-8 x 10^8 exosomes) and cell lysates were subjected to Western blot analysis. The exosomal marker proteins AIP-1, Tsg101, and Flotillin-1 were differently expressed depending on the exosomal donor cell. AIP-1 is most prominent in PrP^C-derived exosomes, whereas PN-derived exosomes also show a high concentration of Flotillin-1. Both cell types release mainly mono- and diglycosylated PrP^C (~30; 35 kDa) via exosomes.

The release of PrP^C on exosomes derived from PrP^C-CL and PrP^C-PN could be shown via western blot analysis (Fig. 6.2). Given that we could not detect an enrichment of flotillin-1 in cell line exosomes as we did in primary neurons exosomes, we suggest that the protein signature of exosomal proteins differs between hippocampal neuronal cell line and primary neurons. However, in both samples the exosomal prion load is mainly made up of mono- and diglycosylated PrP^C in both exosomal samples (Fig. 6.2).

For rescue experiments, the PrP$^{-/-}$ neuronal cell line was transfected with 3F4-tagged PrP^C to generate a stably expressing PrP^{3F4}-CL. Exosomes released by the neuronal cell lines PrP^C, PrP$^{-/-}$, and PrP^{3F4} were characterized by western blot. The 3F4-tagged prion protein was detected with an epitope-specific 3F4-antibody, whereas
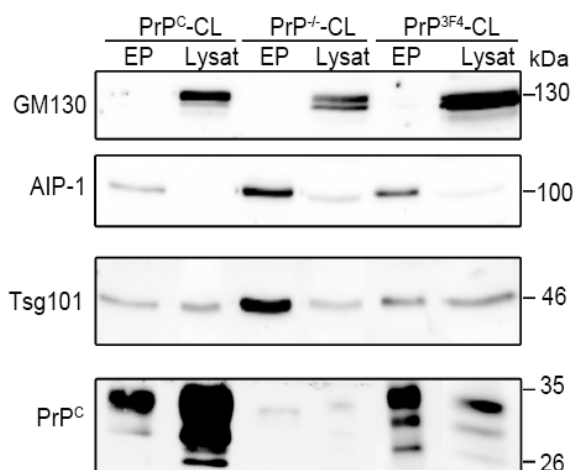
PrP^C was detected using PomII.

Fig.6.3: Western Blot of neuronal cell line – derived exosomes and lysates
Exosomes were purified from supernatants of the Neuroblastoma cell line N2a PrP^C-CL, the prion knockout cell line $PrP^{-/-}$-CL, and the stably 3F4-tagged-PrP^C cell line PrP^{3F4}-CL by serial centrifugation. Exosomal pellets (EP) ($\approx$ 4-8 x 10^8 exosmes) and cell lysates were subjected to Western blot carried out with indicated antibodies. The lysate lane represents 10 µl total lysate of cells from which supernatants were collected. The exosomal marker proteins AIP-1 and Tsg101 are enriched in the exosomal fractions, whereas the Golgi marker protein GM130 was only detected in lysates. Both prion expressing cell lines (PrP^C and PrP^{3F4}) release mainly mono- and diglycosylated PrP^C (~30; 35 kDa) via exosomes.

In western blot analysis of the neuronal cell lines PrP^C, $PrP^{-/-}$, and PrP^{3F4}, it was shown that they release vesicles highly enriched in exosomal marker proteins (AIP-1 and Tsg101) as well as the prion protein, where the diglycosylated form is most prominent, though also monoglycosylated PrP^C was detected in the exosomal fraction of PrP^{3F4}-CL (Fig. 6.3). The Golgi marker protein GM130 was only found in cell lysates demonstrating the purity of those samples.

6.1.2 Sucrose Gradient of PrP^C-CL-exosomes and PrP^C-PN-exosomes

Another method to ensure that the sample contains pure exosomes is a sucrose gradient centrifugation. This method was performed following serial centrifugation. The exosomal preparation was added to continuous sucrose gradient (1,07-1,15 g/cm^3) and during 16 h of centrifugation at 200.000xg the vesicles in the sample will float within a range of sucrose concentration depending on their size and density. These fractions were separately subjected to western blot analysis following SDS-PAGE and analyzed for the exosomal marker proteins (AIP-1 and Tsg101 for neuronal cell line and flotillin-1 for primary neurons) and PrP^C. As a control for

contamination with cell debris, lysate was added to the western blot and GM130 was detected.
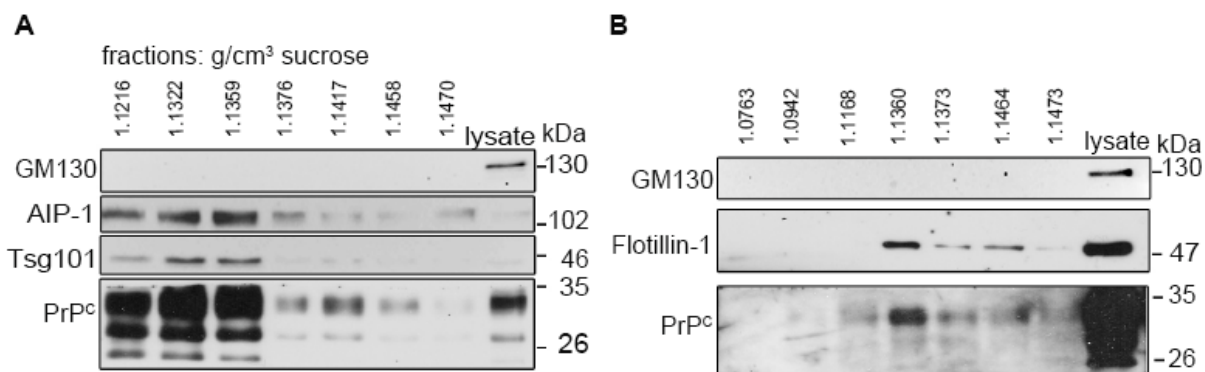

Fig.6.4: Western Blot of PrP^C-CL- and PrP^C-PN exosomes in sucrose fractions
The exosomal preparations were centrifuged for 16 h on a continuous sucrose gradient and subjected to Western blot analysis. (A) Exosomes were purified from supernatants of the Neuroblastoma cell line N2a PrP^C-CL, centrifuged for 16 h on a continuous sucrose gradient and subjected to western blot analysis. PrP^C and exosomal marker proteins AIP-1 and Tsg101 were found in the exosome-typical density fractions. (B) Exosomal pellets derived from wild type primary neurons PrP^C-PN were subjected to western blotting following a sucrose density gradient centrifugation for 16 h. The exosomal marker protein Flotillin-1 and PrP^C were recovered from gradient fractions typical for exosomes.

In the Western blot analysis after sucrose density, the exosomal marker proteins were found in the sucrose density fractions typical for exosomes (1,13-1,19 g/cm^3) (Thery, Ostrowski et al. 2009) for samples isolated out of neuronal cell line PrP^C-CL (Fig. 6.4 A) and primary neuron PrP^C-PN (Fig. 6.4 B) supernatants. Additionally, PrP^C could be detected within these exosomal fractions, thus showing that PrP^C is released via exosomes in the PrP^C-CL and in PrP^C-PN. Consistent with the glycosylation pattern of PrP^C found on exosomes before, the diglycosylated band (~35 kDa) is the most prominent, followed by the monoglycosylated (~30 kDa) and the unglycosylated form of PrP^C (~24kDa) (Fig. 6.4). The quantity of PrP^C on exosomes extracted from cell line supernatants seems to be especially strong when compared to the amount of exosomal marker proteins.

6.1.3 Electron Microscopy of CL-exosomes and PN-exosomes
Determination of exosome size is generally performed via electron microscopy as this method provides the highest resolution power allowing the visualization of even single vesicles can be visualized. To investigate any differences in the shape of exosomes derived from neuronal cell line and primary neurons, exosomes were

harvested from each respective cell culture via serial centrifugation; the pellets were resuspended in 7µl PBS (+PI), placed on 600-mesh carbon-copper grids, negatively stained with 2% uranyl acetate, and examined by transmission electron microscopy.
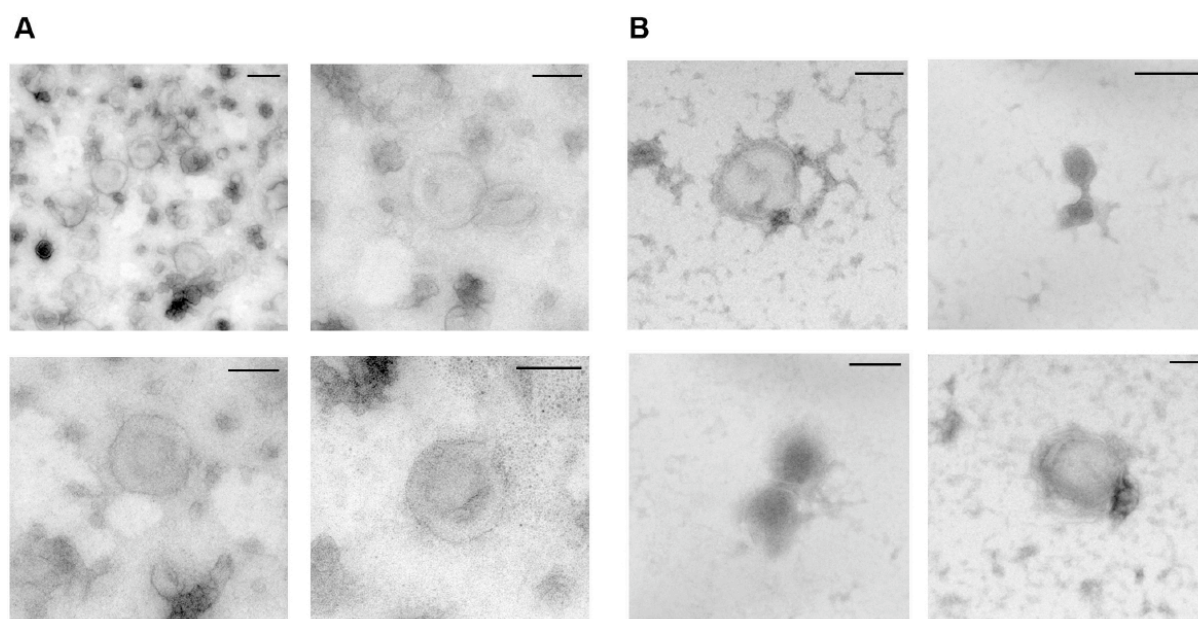

Figure 6.5: Electron Microscopic images of exosomes derived from PrP^C-CL and PrP^C-PN.
Exosomes released by (A) PrP^C-CL and (B) PrP^C-PN were harvested by serial centrifugation, resuspended in 7 µl PBS (+PI), and placed on 600-mesh carbon-coated copper grids. After washing steps, the fixed exosomes were negatively stained with 2% uranyl acetate, dried and examined via transmission electron microscopy. Ultra structural analysis shows cup shaped form of PrP^C-CL-exosomes and PrP-PN-exosomes. The size of analysed exosomes is within 50-100 nm (radius), in which PrP^C-CL-exosomes appear more homogenous in size than PrP^C-PN-exosomes. Scale bars = 100 nm.

The ultra structural analysis via transmission electron microscopy shows a typical cup shaped form of dried exosomes, especially for exosomes released by PrP^C-CL. Their size is about 120 nm in diameter and the average diameter of fixed PrP^C-CL-exosomes appears homogenous within the sample (Fig. 6.5 A). Exosomes released by PrP^C primary neurons (PrP^C-PN-exosomes) appear rather heterogeneous in size, as their diameter ranges from ~70-100 nm (Fig. 6.5 B) and they do not show the cup shape as clearly as PrP^C-CL-exosomes.

After characterization of the samples harvested out of supernatants of cultured cells, it can be concluded that with the help of serial centrifugation exosomes released by neuronal cell lines and primary neurons can be reliably purified. The samples show the exosomal marker proteins (Fig. 6.2/6.3), the typical size (Fig. 6.5) and density

(Fig. 6.3) of typical exosomes in the literature. Furthermore, the exosomes purified contain PrP^C (Fig. 6.3/6.4).

6.2 The Numeric Exosomal Uptake Assay (NEUpA)

In this study, a Numeric Exosomal Uptake Assay was developed, which combines determination of exosomal quantities by static light scattering (see below) and subsequent internalization assay analysed by Flow-cytometry analysis or Confocal Microscopy (see below).

6.2.1 Dynamic Light Scattering of exosomes

In this study, I wanted to determine the requirement of PrP^C content on exosomal or plasma membrane of the recipient cell in the uptake efficiency of exosomes. Therefore, it is necessary to accurately quantify the amount of exosomes harvested from different cell cultures and thus ensure that the same concentration of PrP^C- and PrP$^{-/-}$-exosomes is used in experiments. Uptake efficiencies could then be compared. With DLS and SLS even very small particles can be quantified, as long as these particles are solid in solution at RT during the entire measurement.

To assess whether Light Scattering Techniques can be used to measure exosome concentrations, first Dynamic Light Scattering was performed to receive an impression of the behaviour of exosomes in solution.
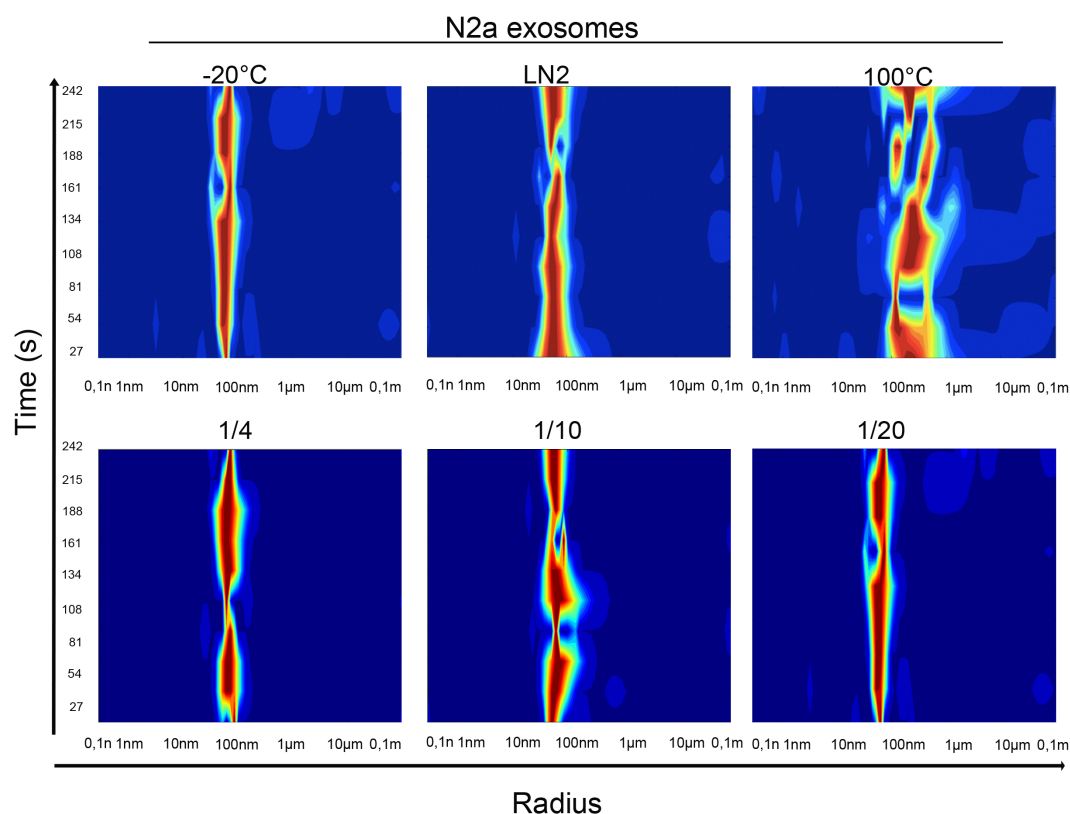
Figure 6.6: Dynamic Light Scattering of N2a derived exosomes.
The diameter of exosomes in solution was determined after freezing exosomes at -20°C or in liquid nitrogen (LN2), boiling (100°C), or diluting 1/4, 1/10, 1/20 in PBS (+PI) previous to measurement.

The mean radius of exosomes in solution was monitored in Dynamic Light Scattering for four minutes after treatment of exosomes (Fig. 6.6). The exosomes appear very robust and stable, as their radius is constant at about 65 nm and does not change even after freezing at -20°C or in liquid nitrogen and thawing, indicating that they do not aggregate or dissolve, unless they are boiled (100°C) (Tab. 6.1). These characteristics of exosomes show that they are suitable for DLS and SLS. Additionally, the count rate (CR) for scattered photons per second (kHz) was determined during each measurement (Tab. 6.1). For most accurate values, the count rate should not exceed 2000 kHz.

Table 6.1: Values of N2a exosomes measured by DLS/SLS.
DLS and SLS were performed after treatment of exosomes as indicated.

Treatment	Radius (nm)	Count Rate (kHz)
-20°C	64,39 +/-5,47	214,9 +/-29,5
LN2	63,66 +/-4,37	192,9 +/-2,8
100°C	219,29 +/-30,83	432 +/-146,2
1/4	70,94 +/-7,59	355,2 +/-37
1/10	66,83 +/- 0,51	488,6 +/-122,1
1/20	65,50	190,7 +/-49,7

6.2.2 Static Light Scattering of exosomes

To determine the absolute concentration (particle/ml) of exosomes in solution, the SLS signal was calibrated by measuring solutions of different concentrations of standardized polystyrene microparticles (100 nm radius) that mimic the radius of exosomes determined by DLS (Tab. 6.2).

Table 6.2: Values of Standard bead solution measured by SLS/DLS.
Listed are density (µg/ml), concentration (particle/ml), and the appropriate CR of a standard bead solution for different dilutions.

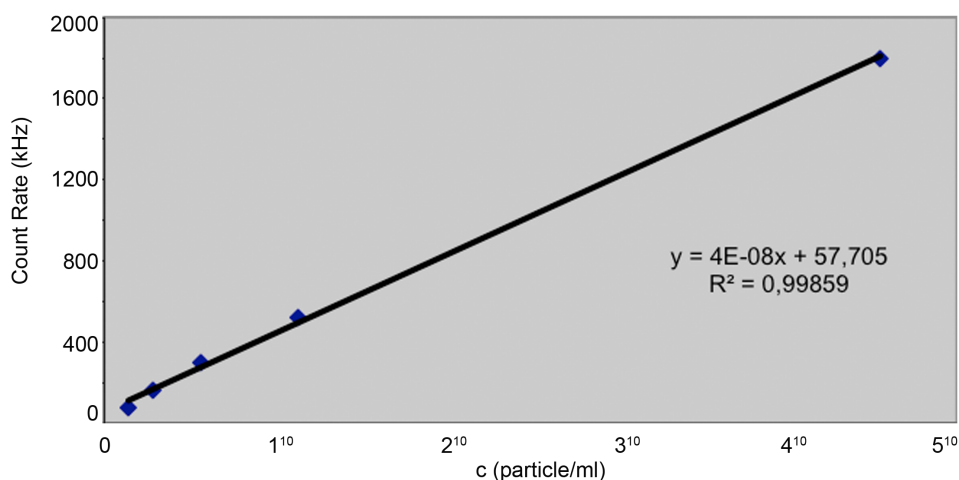| Dilution	µg/ml	particle/ml	Count Rate (kHz)
1000	25	4,55E+10	1800
4000	6,25	1,14E+10	524
8000	3,125	5,69E+09	300
16000	1,56	2,84E+09	160
32000	0,78	1,42E+09	76

$$y = 4E\text{-}08x + 57{,}705$$
$$R^2 = 0{,}99859$$

Figure 6.7: Calibration curve for determination of sample concentrations.
Based on the measurements of a Standard solution, a standard curve was built correlating the count rate to the sample concentration (particle/ml).

For each sample, an accumulation of ten measurements (30 sec each) was performed by an autopilot function, the SLS signal was detected, and by calculations using the standard curve the concentration of exosomes in solution was estimated (Fig.6.7).

Table 6.3: Concentration of N2a exosome samples determined by DLS/SLS.
Pure exosomal fractions were measured as shown above. In comparison to data of the bead standard curve, sample concentrations were calculated.

Sample	Dilution	Mean CR	Stdv.	Concentration (particle/ml)	Mean (particle/ml)
N2a	4	355,20	37	2,97E+10	
	10	488,60	122,10	1,08E+11	
	20	190,7	49,7	6,65E+10	**6,08E+10**

This example shows the general procedure to quantify exosomes via DLS/SLS used in this study. Using this method we quantified exosomes derived from both neuronal cell lines and primary neurons. Since in this method relative exosome concentration (particle/ml) is calculated on the calibration curve valid for particles of 100 nm radius, this calculation represents a suitable estimation, but not an exact quantification. However it remains a very reliable method to prepare equal concentrations of different exosomal samples, which is of outmost important for the set up introduced in this study.
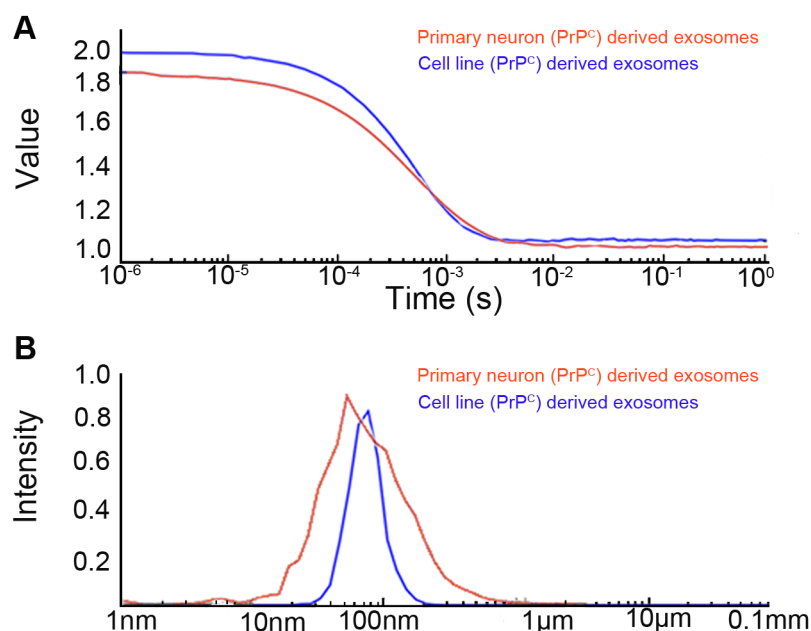
Figure 6.8: Autocorrelation Function and DLS curve.
Autocorrelation Function (A) and DLS curve representing intensities of the respective exosome radius (B) for exosomes derived from PrP^C-CL (blue line) and PrP^C-PN (red line).

The decay of the autocorrelation function (Fig. 6.8 A) shows that the exosomes in solution are in motion. The size distribution for the neuronal cell line and primary neuron derived exosomes reveals a very homogenous radius distribution for PrP^C-CL-exosomes, whereas the PrP^C-PN-exosomes size distribution is a slightly wider. The peaks represent the particle radius for which the signal was most intense. There was no significant difference in the average size of exosomes derived from the cell lines and primary neurons used in this study ($p>0,05$). The average size distribution is listed in Table 6.4.

Table 6.4: Average size distribution of exosomes derived from different origin.
The size distribution in vesicle diameter measured by DLS is listed for exosomes derived from different neuronal cell lines and primary neurons.

Exosome origin	Mean diameter	Stand. Dev.
PrP^C-CL	156	30
$PrP^{-/-}$-CL	140	30
PrP^{3F4}-CL	134	20
PrP^C-PN	124	26
$PrP^{0/0}$-PN	96	16

6.2.3 The Numeric Exosomal Uptake Assay (NEUpA)

Given the possibility to quantify exosomes, a new assay was set up:

Exosomes derived from CL or PN were purified, their concentration was measured by light scattering techniques, and their concentrations were adjusted by diluting with PBS (+PI). Equal amounts of exosomes were then labelled in solution using the fluorescent membrane dye (PKH). Approximately $3x10^8$ labelled exosomes were then co-incubated with confluent recipient PrP^C or $PrP^{-/-}$ cells (in 2ml medium). After 1h of co-incubation, exosomes that were not yet attached or internalized were washed off with ice-cold PBS, the recipient cells were scraped in a final volume of 500 µl PBS (+PI), and kept at 4°C. The amount of fluorescent exosomes taken up in each well was examined by Flow-cytometry using FACSCalibur and data sets were analysed by FlowJo Software. We termed this new method to examine exosomal uptake by recipient cells "Numeric Exosomal Uptake Assay" (NEUpA) (Fig.6.9).
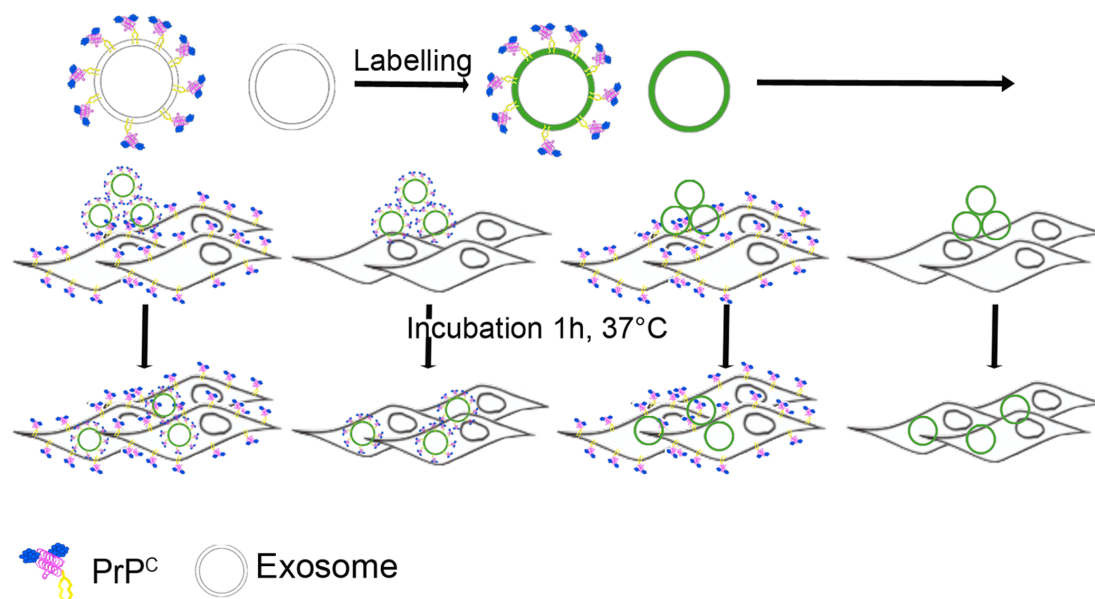
Figure 6.9: Numeric Exosomal Uptake Assay.
Scheme of the Numeric Exosomal Uptake Assay; purified exosomes are labelled (green) and incubated with recipient cell during 1h to asses exosome internalization.
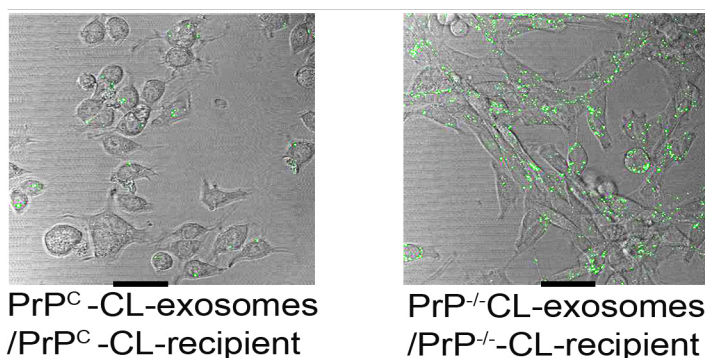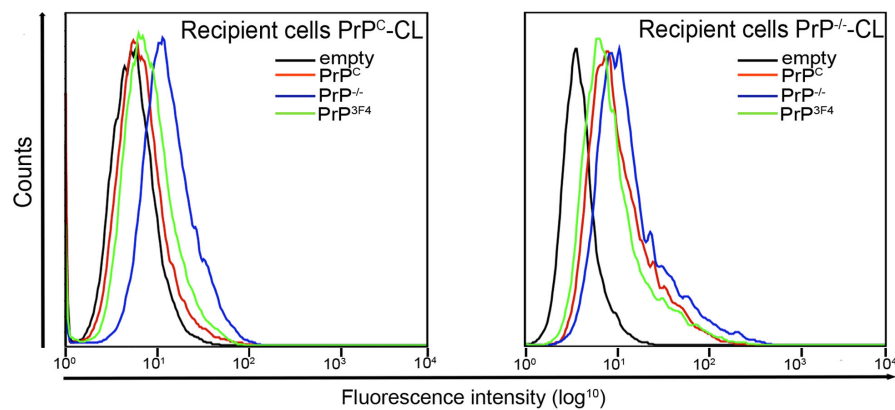

PrP^C-CL-exosomes
/PrP^C-CL-recipient

PrP$^{-/-}$CL-exosomes
/PrP$^{-/-}$-CL-recipient

Figure 6.10: Exosomes taken up by recipient cells.
Exosomes were labelled with PKH dye and incubated with recipient cells for 1h at 37°C. Light-microscopic images show PrP^C-CL-exosomes taken up by PrP^C-CL-recipient cells and PrP$^{-/-}$-CL-exosomes internalized by PrP$^{-/-}$-CL recipient cells. Scale= 41µm

6.3 NEUpA of neuronal cell lines

To assess the PrP^C dependent uptake of exosomes in neuronal cell lines, NEUpA was performed using neuronal cell lines (CL) containing or lacking PrP^C as exosome donors (PrP^C-CL-exosomes; PrP^{3F4}–CL-exosomes; PrP$^{-/-}$-CL-exosomes) and recipients (PrP^C-CL; PrP$^{-/-}$-CL). Following NEUpA, the amount of exosomes taken up was analysed by flow-cytometry and the proportion of uptake efficiency for the resulting combinations (exosomes/recipient cells) was calculated, with the highest uptake efficiency set to 100%.

A

B
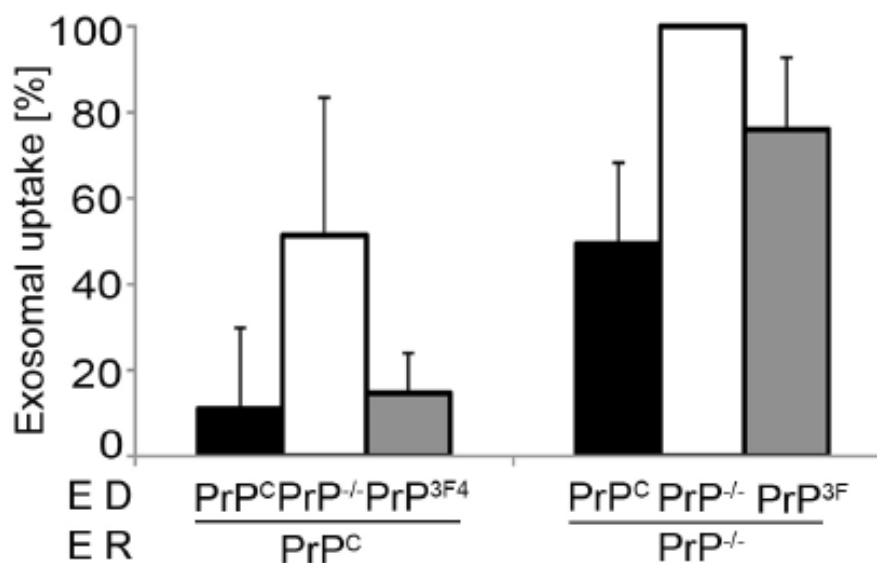
Figure 6.11: Flow-cytometry analysis of NEUpA for CL.
The recipient cell lines PrP^C-CL and PrP$^{-/-}$-CL (ER) were incubated with equal amounts of fluorescently labelled exosomes released by indicated donor cells (ED) for 1h at 37°C (NEUpA) and the exosomal uptake efficiency was determined via flow-cytometry. (A) Representative histograms are shown. (B) Plot reveals the % fluorescence intensity representing the amount of exosomes attached or internalized. Error bars represent the standard deviation (n=3).

The highest internalization or plasma membrane attachment of exosomes was found in the combination PrP$^{-/-}$-CL-exosomes/PrP$^{-/-}$-CL (Fig.10). Presence of PrP^C on either exosomes or recipient cells led to a significant decrease of exosomal uptake. The biggest difference was observed when the uptake efficiency of PrP^C-CL-exosomes by PrP^C-CL-recipient cells was compared to PrP$^{-/-}$-CL-exosomes taken up by PrP$^{-/-}$-CL-recipient cells (p <2,3x10^{-6}; n=3). The exosomal uptake efficiency was ten times lower when prion protein was present (PrP^C-CL-exosomes by PrP^C-CL-recipient cells and PrP^{3F4}-CL-exosomes by PrP^C-CL-recipient cells) (Fig. 6.11). Additionally, when either exosomes or recipient cells lacked PrP^C, the uptake of exosomes was significantly enhanced when compared to wild-type situation (see p-values tab. 6.5). Importantly, the observed effects could be rescued by genetic reintroduction of PrP^C, confirming the specificity of this finding (p-values, table 6.5; n=3).

Table 6.5: P-values for NEUpA of neuronal cell lines.

Exosomes/ Recipient	PrP^C/PrP^C	PrP$^{-/-}$/PrP^C	PrP^{3F4}/PrP^C	PrP$^{-/-}$/PrP$^{-/-}$	PrP^{3F4}/PrP$^{-/-}$
PrP^C/PrP^C	---	0,048*	0,286	2,3x10^{-6}***	0,169
PrP^{3F4}/PrP^C	0,286	0,065	---	4,5x10^{-5}***	0,003**
PrP^C/PrP$^{-/-}$	0,013*	0,465	0,023*	0,005**	0,07
PrP$^{-/-}$/PrP$^{-/-}$	2,3x10^{-6}***	0,03*	4,56x10^{-5}***	---	0,033*
PrP^{3F4}/PrP$^{-/-}$	0,169	0,15	0,0025**	0,033*	---

(n=3; *<0,05; **<0,01; ***<0,001)

6.4 NEUpA of primary neurons

In order to investigate whether these findings also apply to a setting with high *in vivo* relevance, we examined the uptake of exosomes by primary neurons (Fig. 6.12). Therefore, neurons were isolated from wild-type PrP^C and knockout PrP$^{0/0}$ mice at embryonic day 14 (E14) and used in NEUpA. Here the primary neurons served as exosome donors as well as recipient cells. Prior to Flow-cytometry analysis, cells were washed and only cell-bound or internalized exosomes were quantified by Flow-cytometry (Fig. 6.12). Similar to the data obtained by experiments with cell lines, highest uptake was detected for the combination of PrP$^{0/0}$-PN-exosomes incubated

with PrP$^{0/0}$-PN-recipient cells. This value was set to 100% and the uptake efficiency of every combination was calculated.

A
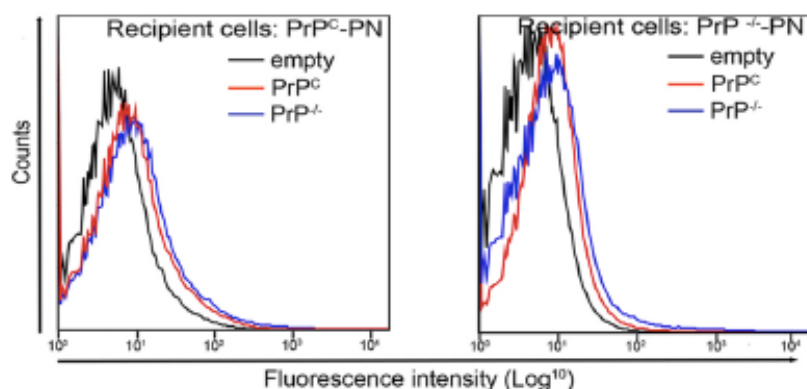
B
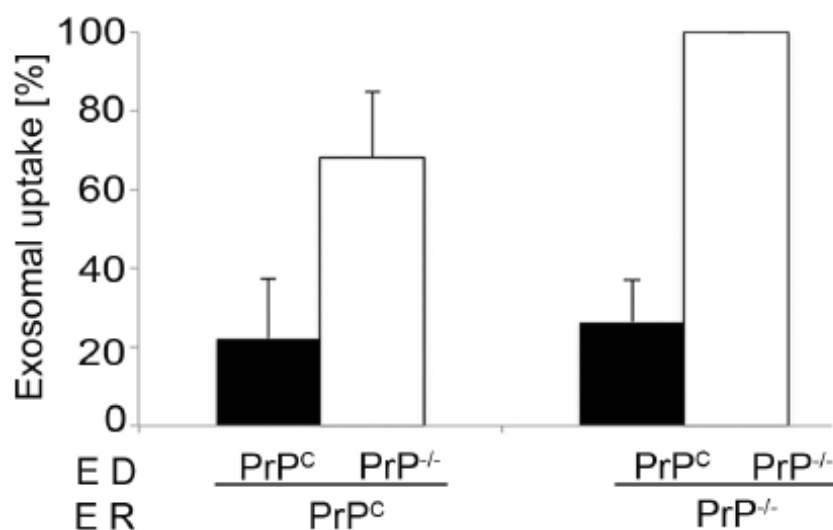
Figure 6.12: Flow-cytometry analysis of NEUpA for PN.
The recipient primary neurons PrP^C-PN and PrP$^{-/-}$-PN (ER) were incubated with equal amounts of fluorescently labelled exosomes released by indicated donor primary neurons (ED) for 1h at 37°C (NEUpA) and the exosomal uptake efficiency (corresponding to the fluorescence intensity) was determined via flow-cytometry. (A) Representative histograms are shown. (B) An average exosomal uptake was calculated (n=3); error bars represent standard deviation.

Table 6.6: P-values for NEUpA of primary neurons.

Exosomes/ Recipient	PrP^C/PrP^C	$PrP^{-/-}/PrP^C$	$PrP^{-/-}/PrP^{-/-}$
PrP^C/PrP^C	---	0,012*	$8,9 \times 10^{-4}$***
$PrP^C/PrP^{-/-}$	0,359	0,034*	$2,9 \times 10^{-4}$***
$PrP^{-/-}/PrP^{-/-}$	$8,9 \times 10^{-4}$***	0,03*	---

(n=3; *<0,05; **<0,01; ***<0,001)

Also *in vivo* expression of PrP^C on either exosomes or recipient primary neurons lead to a statistically significant decrease of exosomal uptake (p-values, tab. 6.6). The uptake efficiency of exosomes was almost five times lower for Prion Protein containing conditions (PrP^C-PN-exosomes/PrP^C-PN = 22%). Consistent with the results obtained utilizing cell lines (above), the strongest difference in exosomal uptake efficiency was found for PrP^C-PN-exosomes/PrP^C-PN**::**$PrP^{-/-}$-PN-exosomes/$PrP^{-/-}$-PN (p=$8,9 \times 10^{-4}$).

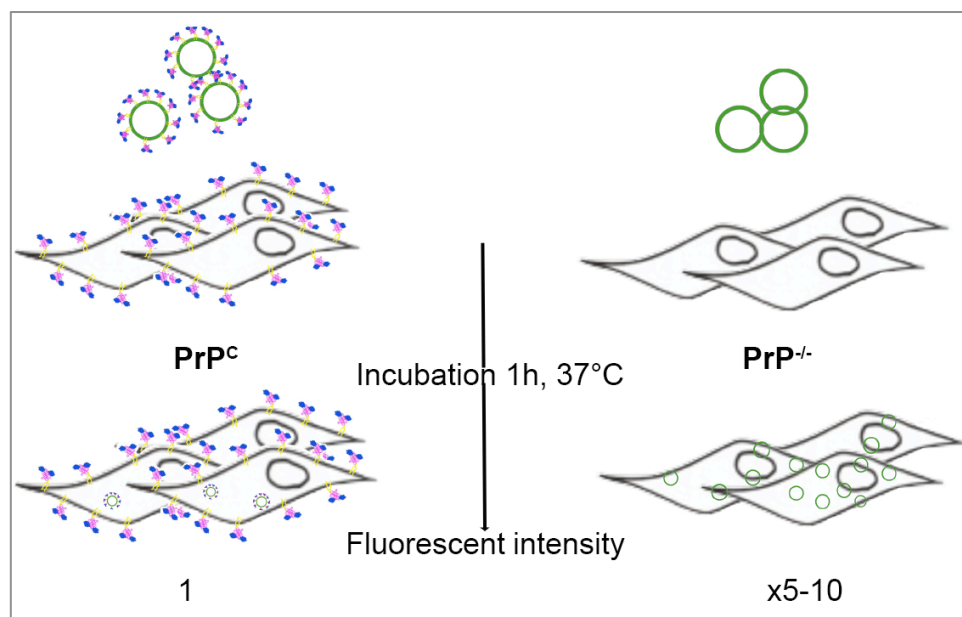**Figure 6.13: PrP^C dependent NEUpA of neuronal cell lines and primary neurons.**
Scheme summarising the PrP^C dependent exosomal uptake efficiency measured by Numeric Exosomal Uptake Assay (NEUpA) and Flow-cytometry for PrP^C containing and PrP^C lacking ($PrP^{-/-}$) conditions in primary neurons (x5 for $PrP^{-/-}$) and neuronal cell lines (x10 for $PrP^{-/-}$).
=PrP^C; ◯=green-fluorescent labelled exosome

With the help of the newly generated NEUpA, exosomal uptake efficiencies could be quantified, revealing a strong impact of PrP^C depletion. It was found that PrP^C decreases the amount of exosomes taken up by recipient cells after 1h compared to the knockout condition (Fig. 6.13).

6.5 Analysis of PrP^C dependent intracellular trafficking of exosomes

As PrP^C has been shown to be involved in internalization processes such as phagocytosis (de Almeida, Chiarini et al. 2005; Nitta, Sakudo et al. 2009) in previous studies and we now show an involvement of PrP^C in the exosomal uptake or plasma membrane attachment efficiency, we hypothesised that PrP^C influences intracellular trafficking by directing exosomes to a specific route of endocytosis.

6.5.1 Analysis of intracellular trafficking using Immunofluorescence

To address this question, about $3x10^8$ exosomes from neuronal cell lines expressing or lacking PrP^C were used in NEUpA with neuronal cells expressing or lacking PrP^C serving as recipient cells (in 2 ml medium). The exosomes were co-incubated with the recipient cells for 15 minutes, cells were washed and the internalized or attached exosomes were allowed to follow an intracellular traffic route within 1 additional hour of incubation ($37°C$, $5\%CO_2$). Cells were fixed and early recycling compartments (Rab4) or late endosomes and lysosomes (LBPA) were immuno-fluorescently labelled and analysed by Confocal Microscopy. The amount of co-localization of internalized exosomes (green) and the particular endosomal compartment (red) (Fig. 13) was determined taking consecutive z-stacks and analysed with ImageJ Software. The resulting graph was obtained by two independent experiments (= 5 coverslips) (Fig. 6.14 B).

A

B
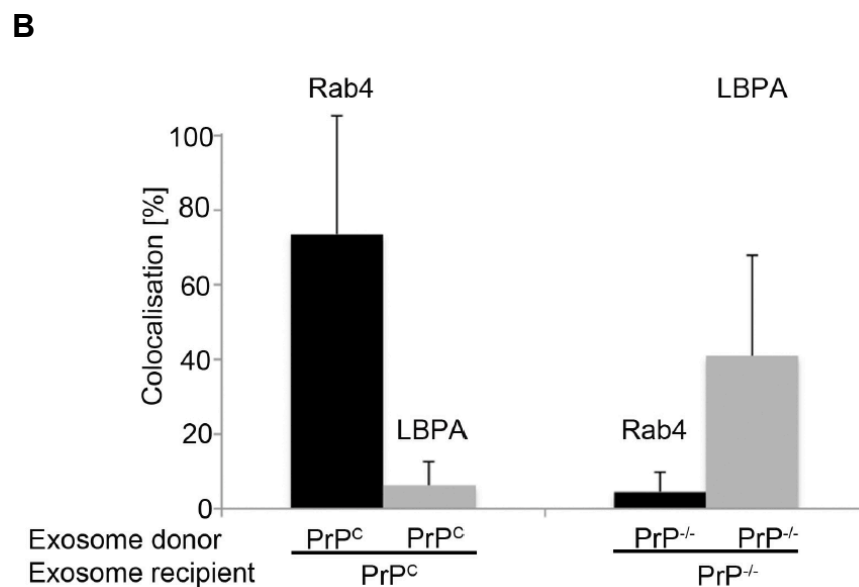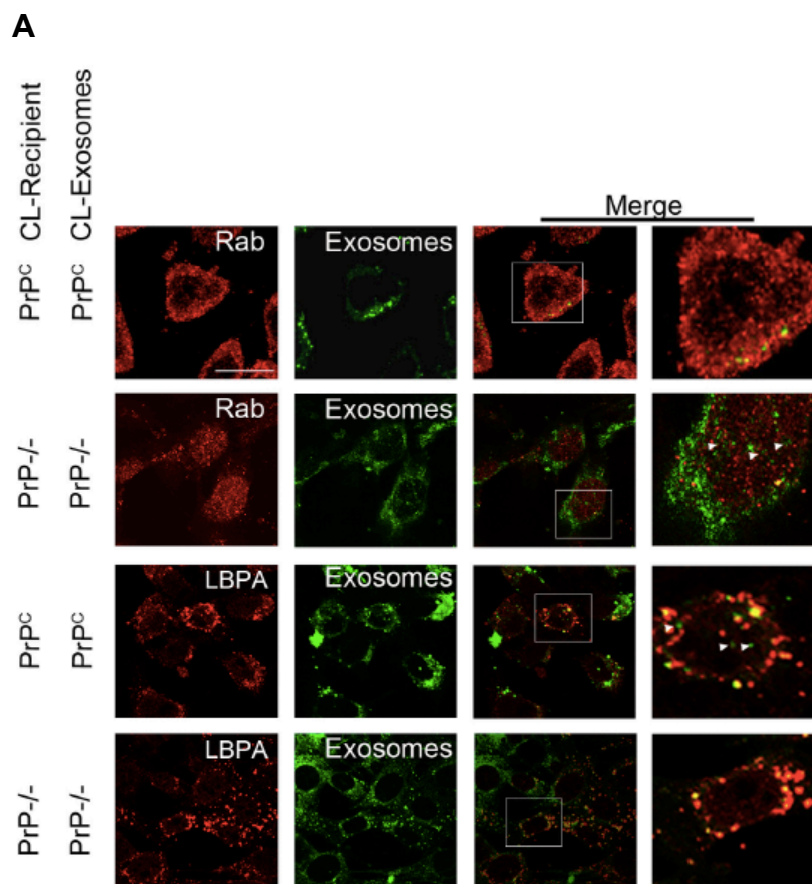
Figure 6.14: PrP^C dependent internalization of exosomes.
Fluorescently labelled exosomes (green) (PrP^C and PrP$^{-/-}$) were co-incubated with recipient neuronal cells (PrP^C and PrP$^{-/-}$) for 1h of internalization (37°C). After internalization, cells were fixed and compartments (early recycling endosomes = Rab4; late endosomes and lysosomes = LBPA) were immune-fluorescently labelled (red). (A) Z-stacks of recipient cells were taken and representative Confocal Microscopy images (one z-level) are shown. Exosomes co-localizing with the compartment of interest appear yellow whereas white arrowheads indicate exosomes

that are not incorporated by the compartment of interest. Scale bar= 10 µm. (B) The percentage of co-localizing exosomes out of all internalized exosomes was calculated for the specific endocytic compartment. The error bar represents the standard deviation (= 5 coverslips, 2 independent experiments).

In the presence of PrP^C, exosomes are found to mainly co-localize with early recycling endosomes (74% co-localization with early recycling endosomes containing Rab4 compared to only 6% co-localization with LBPA positive late endosomes and lysosomes), whereas $PrP^{-/-}$-CL-exosomes predominantly co-localize with late endosomes and lysosomes (41% co-localization with LBPA compared to only 4,5% co-localization with Rab4). These results show that seven times more exosomes are incorporated by late endosomal compartments after 1h of endocytosis when PrP^C is missing (Fig. 6.14 B). This finding indicates that PrP^C influences exosomal trafficking and retains exosomes in Rab4 containing early endosomal compartments while $PrP^{-/-}$-CL-exosomes are transported to late endosomes and lysosomes instead.

6.5.2 Analysis of intracellular trafficking using life cell imaging

To get a better insight into the kinetics of recruitment into lysosomes I utilized a live cell imaging system in combination with LysoTracker. Lysosomes and acidic compartments were labelled with 75 nM LysoTracker while the nucleus was labelled with 2 µg/ml Hoechst for 20 minutes. Fluorescently labelled exosomes containing 3F4-epitope tagged PrP^C (PrP^{3F4}) were incubated with PrP^{3F4}-CL recipient cells for 30 minutes. Next, the medium was exchanged with 37°C exosome-free DMEM and exosomal endocytosis was monitored (Fig .6.15 A) for additional 35 min (three spots x 5 time points, each dish). The percentage of exosomes taken up by acidic compartments was calculated (Fig. 6.15 B).

A

PrP^(-/-)-CL-exos/PrP^(-/-)-CL

PrP^(3F4)-CL-exos/PrP^(3F4)-CL

B

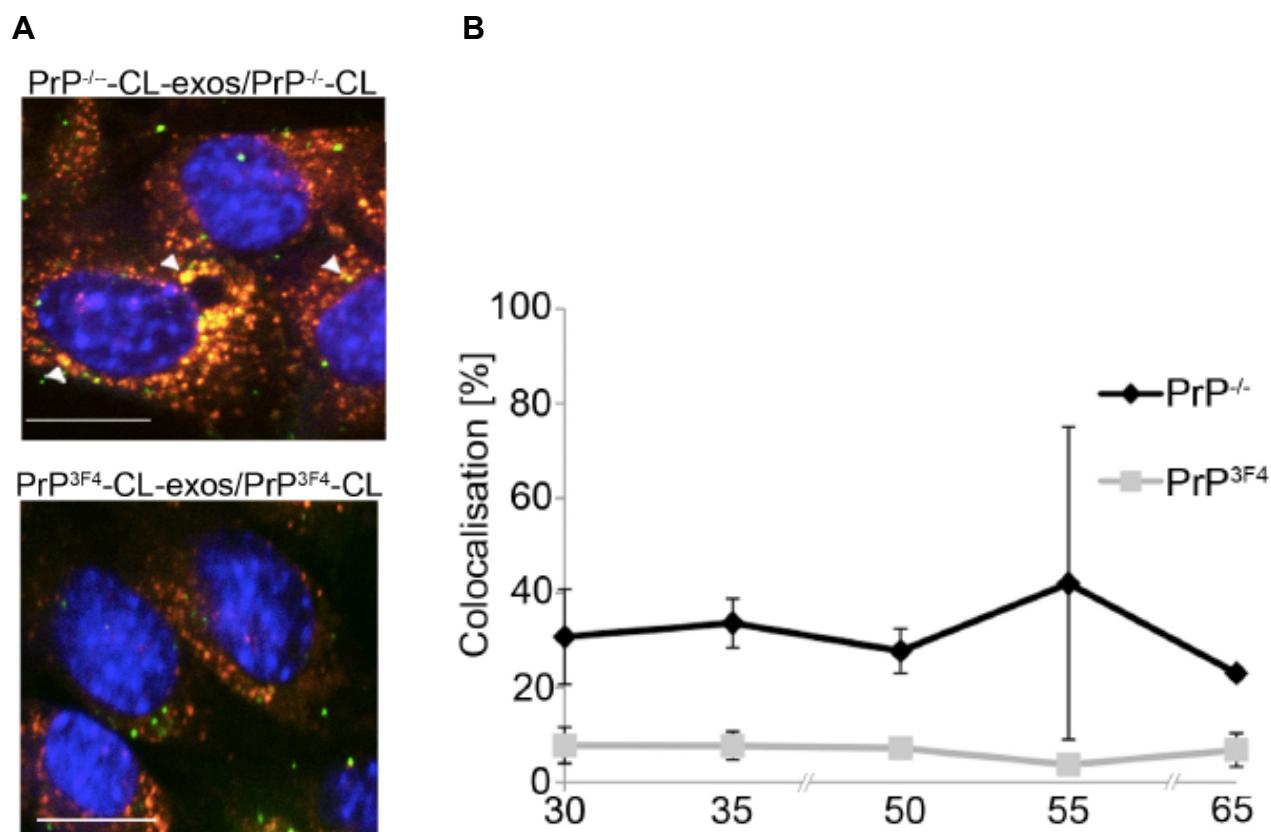**Figure 6.15: PrP^C dependent entry into the degradation pathway of exosomes.**
Fluorescently labelled exosomes (green) containing PrP^C (PrP^{3F4}) and lacking PrP^C (PrP$^{-/-}$) were co-incubated with PrP^{3F4}-CL or PrP$^{-/-}$-CL recipient cells (labelled with LysoTracker red) for 30 minutes. In the last 20 min of incubation 2 µg/ml Hoechst342 was added to the medium to stain the nuclei (blue). Then non-attached or internalized exosomes were washed off with PBS, warm medium was added and the endocytic route of already internalized exosomes was followed by confocal microscopy for 35 minutes with life imaging confocal microscopy. (A) Representative confocal images of internalized exosomes (green) and LysoTracker (red). White arrowheads indicate big acidic compartments in co localization (yellow) with exosomes. Scale bar= 25 µm. (B) The percentage of exosomes co-localizing with LysoTracker red in the recipient cell line was calculated for 35 min (5 time points). Three different spots (á≈5 cells) were scanned at every single time point by acquiring z-stacks. Scale bars representing the standard deviation. During the entire measurement ~10% of all PrP^{3F4}-CL exosomes taken up by PrP^{3F4}-CL recipient cells, co localised with LysoTracker. The co localisation of PrP$^{-/-}$-CL-exosomes with PrP$^{-/-}$-CL-recipient cells was more than three times higher. Error bars represent the standard deviation between three spots analysed in one experiment.

Table 6.7: Co localization [%] of PrP^C-CL-exosomes and PrP^{3F4}-PN-exosomes with LysoTracker. The amount of exosomes co localising with LysoTracker [%] is listed.

Time [min]	PrP^{3F4}/PrP^{3F4}	PrP$^{-/-}$/PrP$^{-/-}$
30	7,8	30,7
35	7,7	33,6
50	7,2	27,7
55	3,7	42
65	6,8	23

Following the exosomal transport to lysosomes by life cell imaging while tracking late endosomes and lysosomes via LysoTracker (which stains acidic compartments in red), it could be shown that PrP^C delays the entry of exosomes into lysosomes, presumably to follow a degradation pathway. In the presence of PrP^C (PrP^{3F4}) on exosomes and recipient cells, less than 10% (Tab. 6.7) of all exosomes taken up co localize with late endosomal compartments, whereas up to 42% (Tab. 4.7) of exosomes co localize with late endosomes and lysosomes when PrP^C is knocked out (PrP$^{-/-}$) (Fig. 6.15).

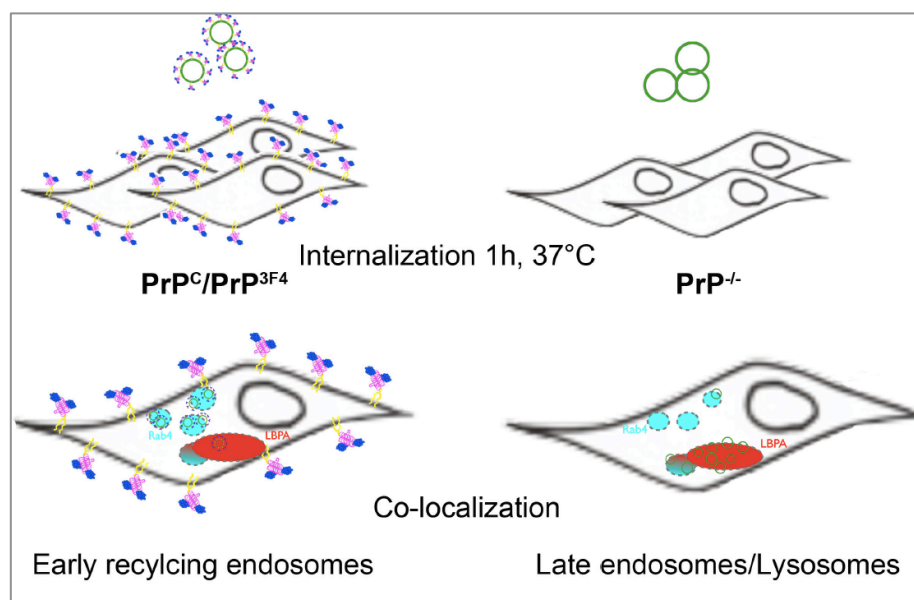**Figure 6.16: PrP^C dependent intracellular trafficking of exosomes.**
Scheme summarising the PrP^C dependent endocytic transport of exosomes. In Numeric Exosomal Uptake Assays exosomes retain in early endocytic compartments in PrP^C containing conditions; in PrP$^{-/-}$ conditions, exosomes mainly co-localize with late endosomes and lysosomes after 1h of endocytosis.
=PrP^C; ⚬=green-fluorescent labelled exosome

With the investigation of the NEUpA, the uptake efficiency of exosomes by recipient cells could be quantified via Flow-cytometry. Additionally, the endocytic pathway of exosomes could be visualized using confocal microscopy. It was found that the attachment and internalization of exosomes in neuronal cell lines and primary neurons was decreased in the presence of PrP^C. Furthermore, more exosomes are taken up by late endosomes and lysosomes when PrP^C is knocked out compared to wild type situations in which PrP^C is present in which where exosomes co localise with early recycling endosomes (Fig. 6.16).

6.6 Endocytosis of transferrin in neuronal cell lines

To investigate whether the PrP^C –dependent effects on exosomal internalization result from common changes in endocytosis, the neuronal cell lines were checked for differences in endocytosis. Since the transport of exosomes to Rab4 positive recycling endosomes is different in PrP^C-, $PrP^{-/-}$-, and PrP^{3F4}-CL, the uptake of transferrin was examined as it is endocytosed and recycled via Rab4-positive endosomes. A possible common alteration in Rab4-mediated endocytosis should be reflected in altered transferrin internalization. PrP^C-, $PrP^{-/-}$-, and PrP^{3F4}-CL were grown to ~70% confluence, 5 µg/ml AlexaFluor594-labeled holotransferrin (in cell culture medium) was added, and allowed to be internalized by the neuronal cells for 1h at 37°C. Incubation was stopped (4°C), the cells were washed with cold PBS, and fixed (4% Paraformaldehyde). Next, the internalization of transferrin was determined taking consecutive z-stacks and analysed with ImageJ software (Fig. 6.17).
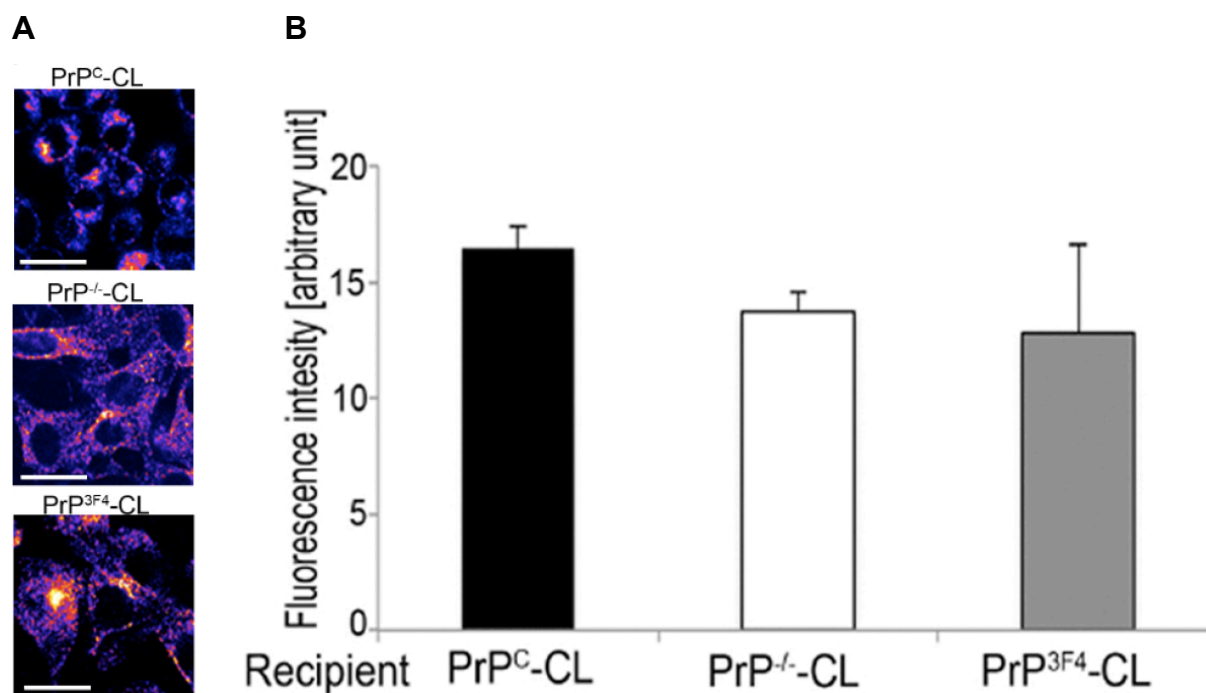
Figure 6.17: PrP^C dependent endocytosis of transferrin.
Confluent neuronal CL (PrP^C-, PrP$^{-/-}$-, and PrP^{3F4}-CL) were incubated with 5 µg/ml AlexaFluor596-labeled holotransferrin (in cell culture medium) for 1 h at 37°C, 5% CO_2 allowing internalization by recipient cells. Consecutive z-stacks (Leica Laser Scanning Confocal Microscope TCS Sp2) were taken after washing (2 times cold PBS) and fixation (4% Paraformaldehyde) of the cells. Representative confocal images are shown from different z-levels (A). Scale bar= 10 µm. The transferrin uptake was measured by fluorescence intensity per cell volume for respective CLs and analysed using ImageJ software (B). Error bars represent standard deviation between three coverslips. No significant difference could be observed for the uptake of transferrin in neuronal-CL (p>0.5).

Utilizing the transferrin uptake to examine classical Rab4-dependent endocytosis, no significant difference could be observed for PrP^C-, PrP$^{-/-}$-, and PrP^{3F4}-CL, indicating that the differences in exosomal uptake are not due to a common change in Rab4-dependent endocytosis, but due to a specific alteration of the internalization of exosomes.

7   DISCUSSION

In this study the role of the cellular prion protein (PrP^C) in exosomal trafficking was examined as a possible novel physiological function for PrP^C. Before the beginning of this project, it was known that PrP^C is highly abundant on exosomes (Fevrier, Vilette et al. 2004) and that PrP^C as well as PrP^{Sc} can be transported via exosomes, which can spread prion infectivity with high efficiency (Leblanc, Alais et al. 2006). Since exosomal internalization might involve receptor-mediated mechanisms and PrP^C has been shown to interact with several plasma membrane proteins, a possible role for PrP^C within this uptake mechanism was hypothesized. Furthermore, the release of PrP^C-containing exosomes by neuronal cells has been previously demonstrated. Intercellular communication is of great importance between neuronal cells. In fact, it has been shown that exosomes mediate transport of protein, lipids, and small ribonucleic acids (RNAs) between several cell types, including neurons (Thery, Ostrowski et al. 2009). Therefore, the potential function of PrP^C in exosomal uptake by neurons offers an intriguing new possibility for the physiological function of PrP^C and opens a very interesting field of research. In contrast to previous studies on exosomal internalization by recipient cells, we did not block general endocytic pathways, because these techniques usually altered the entire vesicular trafficking system and could result in indirect exosomal defects (Feng, Zhao et al. 2010; Fitzner, Schnaars et al. 2011). In order to directly investigate the role of PrP^C in exosomal uptake, this study examines the exosomal uptake of PrP^C- and PrP$^{0/0}$-primary neurons and PrP^C-, PrP$^{-/-}$, and PrP^{3F4}-neuronal cell lines. The observed effects are caused by differences in PrP^C expression directly as the PrP$^{-/-}$-phenotype could be rescued by PrP^{3F4}-transfection. A new method to quantify exosomal uptake efficiency and intracellular transport of exosomes (NEUpA) was designed and a novel physiological function of PrP^C was found.

7.1   Pure exosomal fractions were derived from neuronal cell lines and primary neurons

To purify exosomes from cell culture supernatant an established method of serial centrifugation steps was used, which should result in pure exosomal preparations. To ensure that the protocol was sufficient with the cells used in this study, the samples were characterized after purification. Indeed, purified exosomes showed the typical exosomal density, a cup-shaped or round structure in transmission electron

micrographs, and contained typical exosomal marker proteins. Exosomes are small membrane vesicles of endosomal origin released by the fusion of multivesicular bodies (MVBs) with the plasma membrane of the donor cell. Depending on their originating cell, they contain cell-specific protein and lipid signatures. There is no exosome-specific protein, which is excluded from other vesicles. However, the characteristics of exosomes are unique. The biogenesis of exosomes within the endocytic pathway is mediated at least in part by ESCRT-complexes, which are involved in the synthesis of MVBs and the sorting of proteins within these structures. The vesicles harvested in this study show an enrichment of these ESCRT-proteins on a western blot analysis (Fig. 6.2/6.3), supporting MVB-derived exosomal biogenesis. In addition to ESCRT-proteins lipid-raft-proteins can serve as exosomal markers. In fact, exosomes are highly enriched in lipid-raft-domains. In this study, vesicles released by primary neurons showed an enrichment of flotillin-1 (a constituent of lipid sub-domains in recycling endosomes and lipid-rafts in the plasma membrane) whereas flotillin-1 could not be detected in the exosomes from neuronal cell line (Fig. 6.2). This finding suggests that a different membrane composition characterizes these two groups of exosomes, possibly with a higher amount and/or different protein composition of their lipid-raft-domains. PrP^C can be clearly detected in cell line-derived exosomes despite the lack or decrease levels of flotilin-1 and possibly of lipid-raft domains. This observation suggests that exosomes derived from cell lines contain a distinct protein composition. This difference could have its origins in the mechanism of exosome biogenesis, which might also result in different subgroups of exosomes released by a single cell line. For instance, initial budding of the plasma membrane during exosomal biogenesis could be different between neuronal cell lines and primary neurons. Alternatively, flotillin-1 on exosomes may not originate exclusively from the plasma membrane where lipid-raft domains are abundant, but may be enriched during maturation of ILVs in a similar way as it has been shown for the maturation of phagosomes (Dermine, Duclos et al. 2001). In fact, PrP^C in neuronal cell lines can move towards less ordered domains, where it can bind to the low-density lipoprotein receptor-related protein 1 (LRP1) to be endocytosed via coated pits (Parkyn, Vermeulen et al. 2008). Thus, PrP^C is not only found within lipid-raft domains. An alternative endocytic route for PrP^C independent of classical receptor mediated endocytosis could be mediated by non-coated pit endocytosis that may be driven by the aggregate properties of lipid rafts and by yet

unknown mechanisms (Miesbauer, Rambold et al. 2010). So far it is not known by which mechanism vesicles get enriched in raft-domains, but is likely to happen at the stage of ILV generation, as they contain a higher amounts of cholesterol and sphingomyelin (Stoorvogel, Kleijmeer et al. 2002). These data indicate that the sorting of proteins and lipids into exosomes is highly protein- and cell type-specific. Many proteins are specifically sorted into ILVs during multivesicular body formation. This is largely mediated by endosomal proteins containing an ubiquitin-interacting motif (UIM) (Hofmann and Falquet 2001; Bilodeau, Urbanowski et al. 2002; Raiborg, Bache et al. 2002), which can interact directly with ubiquitinated cargo, or adaptor proteins. The ESCRT-protein Tsg101 contains an ubiquitin E2 variant (UEV) domain, which can also bind ubiquitin with low affinity (Pornillos, Alam et al. 2002). The presence of Tsg101 in exosomes released by neuronal cell lines and primary neurons suggests a possible role of ubiquitin-binding proteins in sorting of cargo into ILVs in these neuronal cells. Still it is more likely that PrP^C and PrP^{Sc} are transported to ILVs in an ubiquitin-independent way as it has been shown for mammalian LRP1 (Reggiori and Pelham 2001). In contrast to a study on Rabbit kidney epithelial (RK13) cells and neuronal GT1-7 cells in which less monoglycosylated PrP^C was released on exosomes (Vella, Sharples et al. 2007), this study found no different ratio between PrP-glycotypes released via exosomes derived from wild-type (N2a) and Prion-transfected (PrP^{3F4}) neuronal cell lines and primary neurons (Bl6, wild-type). The exosomal glycopattern of PrP^C was comparable to the PrP^C-glycopattern of the plasma membrane showing strong abundance of diglycosylated PrP^C. Thus, the GPI-anchor-driven clustering of PrP^C into lipid-rafts might favour incorporation of un-, mono- and diglycosylated PrP^C into ILVs as it does for other GPI-anchored proteins (Simons and Ikonen 1997). Another possible mechanism of sorting PrP^C into exosomes might be the cleavage of PrP^C by ADAM10, which is the sheddase of PrP^C (Altmeppen, Prox et al. 2011) and has been shown to actively sort CD23 (a lectin) into exosomes (Mathews, Gibb et al. 2010).

On electron micrographs the cell line (CL)-derived exosomes appear cup-shaped and bigger than exosomes derived from primary neurons (PN). This difference in structure is probably due to a different drying behaviour during the staining process as a result of different lipid-compositions. The focus of this study was to understand the internalization of exosomes released by these neurons. However it will be very interesting to analyse the exosomes further and reveal their exact protein- and lipid

composition, which might reveal in more detail the different pathways and mechanisms of exosome-biogenesis.

7.2 The Numeric Exosomal Uptake Assay (NEUpA)

To assess the function of PrP^C in exosomal internalization and intracellular trafficking, a new method was established to quantify exosomal uptake efficiency and visualize exosomal pathways. In the Numeric Exosomal Uptake Assay (NEUpA), exosomes are quantified using light scattering techniques and a specific amount of fluorescent exosomes is then applied to uptake experiments. Following uptake experiments, the efficiency of exosomes taken up by recipient cells could be calculated using flow-cytometry.

Due to the small size of exosomes (~120 nm), it is very hard to track or visualize a single vesicle and determine a final concentration. Here, light scattering techniques represent a very useful solution as they can track and count even single macromolecules ($\leq$ 1 µm). In dynamic light scattering (DLS, or photon correlation spectroscopy) the emission of light by oscillating particles in solution is detected, measuring the particle size and their hydrodynamic diffusion coefficients (Chu 1997). After calibration to the desired radius range, the concentration of exosomes in solution was measured using the signal (kHz) determined by static light scattering (SLS). The entire procedure is fast and can be performed at room temperature, as no change in the structure of exosomes could be observed, as but they still appear round and with a constant diameter (Fig. 6.6). We conclude that the quantification protocol did not alter exosomal biophysical characteristics and as a result they could be applied in uptake assays. The concentration for exosomes in solution measured by DLS and SLS is determined by comparison to a calibration curve (Fig. 6.7) and thus is not an exact quantification, but an approximation to the exact value. It is a very reliable method to match samples concentrations of different origin and it is crucial for the NEUpA. No significant differences in size distribution could be observed between exosomes derived from neuronal cell lines and primary neurons (Tab. 6.4), no significant difference could be observed between cell lines and primary cells. In the DLS curve (Fig. 6.8), the average size distribution of exosomes derived from primary neurons is wider than for those derived from neuronal cell lines. This is probably due to the variety of cell types and sizes in primary neuronal cultures compared to similar cells within one cell line that is generated out of a clonal line. In

agreement with other studies, exosomes in solution show a bigger diameter in DLS/SLS, than in scanning electron microscopy (Fig. 6.5), with an average 130 nm (Tab. 6.4) (Sokolova, Ludwig et al. 2011). Hence, exosomes can be quantified via DLS and SLS at room temperature without losing structural integrity during the procedure, which is the basis of the NEUpA.

7.3 PrP^C decreases the uptake of exosomes

Using NEUpA, the uptake efficiencies of exosomes could be analysed by flow-cytometry as the fluorescent intensity of the cells correlates with the amount of exosomes taken up by the recipient cells or attached to its plasma membrane. Previous published studies on exosomal transport were often performed with fibroblast or macrophage cell lines, which show a high exosomal transport activity. However, the amount of exosomes used in internalization studies was never calculated. These publications only revealed the amount of exosome protein or the number of cells releasing the exosomes. Despite the fact that exosomes were derived from similar amounts of cells, we could not find a reliable exosomal marker protein with equal levels throughout different cell types. In fact, even the ratio of the marker proteins to each other seemed to change. As a result, light scattering techniques were used to quantify the exosome concentrations in the samples used for an uptake assay. Thus, in this study for the first time internalization of a known number of exosomes could be analysed (NEUpA). To reveal the impact of PrP^C in the exosomal uptake of neurons, labelled exosomes (PrP^C or PrP$^{-/-}$) were incubated with recipient neurons (PrP^C or PrP$^{-/-}$) allowing internalization for 1h, as internalization of exosomes increases during the first hours of incubation (Feng, Zhao et al. 2010). After co incubation with recipient cells, internalization was stopped by placing samples at 4°C. Instead of washing the samples with an acidic solution that would strip bound exosomes from the plasma membrane, cells were washed several times with PBS. In this way exosomes that were not attached to the plasma membrane were removed, but exosomes bound to the plasma membrane due to eventual recycling processes could be captured by flow-cytomeric analysis. By comparing the exosomal uptake efficiencies of neuronal cell lines and primary neurons in dependence of PrP^C, it was demonstrated that PrP^C significantly decreases the amount of exosomes taken up or bound to the plasma membrane (Fig. 6.12). The altered exosomal uptake in PrP$^{-/-}$-cells could be rescued to wild type

by transfection of PrP^C, demonstrating the specificity of the phenotype for PrP^C. The alteration was shown to be exosome-specific and independent from a general alteration in endocytosis since transferrin uptake is similar in the cell lines and independent of PrP^C. This drastic effect is most likely due to a higher internalization of exosomes as no accumulation at the plasma membrane could be observed in confocal microscopy. Additionally it might be enhanced by a higher exosome-recycling rate in wild-type neurons. Moreover no fusion with the plasma membrane could be observed, but exosomes rather appear intact after uptake indicating a phagocytic internalization mechanism as it has been postulated for different cells before (Feng, Zhao et al. 2010). The new findings may help to explain functions of PrP^C in phagocytosis since phagocytosis of model substrates is enhanced in macrophages of PrP$^{0/0}$-mice (de Almeida, Chiarini et al. 2005).

7.4 PrP^C retains exosomes in early recycling compartments

Interestingly PrP^C on the exosomal or plasma membrane inhibits the uptake of exosomes, pointing to a way of exosomal internalization involving PrP^C interacting with a plasma membrane protein decelerating and eventually defining the uptake. To clarify the role of PrP^C in the process of exosomal uptake, their fate within recipient cells was visualized and co localization with endocytic compartments was analysed by confocal microscopy following NEUpA. The high accumulation of PrP^C-exosomes in early recycling compartments (Fig. 6.13) indicates that PrP^C retains exosomes in early endosomal compartments and even favours their recycling or that a high amount of exosomes internalized triggers targeting to lysosomes whereas low numbers of exosomes are retained in early endosomes. However, this finding might explain the high rate of transmissibility of PrP^{Sc} via exosomes since the conversion of PrP^C is thought to occur in early endosomal compartments (Marijanovic, Caputo et al. 2009) and exosomes represent a mechanism to bring the two prion conformers together and support pathogenic interaction (Morris, Parkyn et al. 2006). Studies on the uptake efficiency of exosomes bearing PrP^{Sc} by PrP^C- and PrP$^{-/-}$-cells and their endocytic route might reveal deeper insight into that mechanism.

7.5 Impact of the results gained in this study

In non-infected organisms, this specific way of internalization and targeting to early recycling endosomes is a great advantage for the tissue, because signalling

cascades are probably induced in the early phases of exosome attachment or internalization as the exosomal membrane proteins may interact with plasma membrane receptors or exosomes may release RNA upon fusion to the recipient cell (von Zastrow and Sorkin 2007; Rani, O'Brien et al. 2011). Exosomes represent a communication vector from cell to cell and from tissue to tissue. Since they were found to transfer small ribonucleic acids (RNAs) such as microRNAs (or exosomal RNA (esRNA) they were shown to influence gene expression of target cells (Ramachandran and Palanisamy 2011). Also lipids and proteins are not exclusively targeted to recipient cells for degradation, but their transport is very important in communication between cells. Especially between immune cells the transfer of functional proteins appears to be very common, thus exosomal transport has been studied intensely in cells of the immune system (Davis 2007; Mathews, Gibb et al. 2010). The formation of peptide-MHC class II complexes (pMHC-II) and its interaction with the T-cell receptor (TCR) is required for the interaction between B-cells or dendritic cells (DCs) and antigen-specific T-cells, which is essential for the activation of an efficient immune response (Davis, Boniface et al. 1998). It has been shown that exosomes hold an important role in the activation of T-cells by delivering antigens from B-cells or DCs to naive T-cells and induce an immune answer *in vitro* and *in vivo* (Zitvogel, Regnault et al. 1998; Thery, Duban et al. 2002; Segura, Amigorena et al. 2005; Segura, Nicco et al. 2005). Exosomal release of pMHC-II is a mechanism, which allows pMHC-II to escape from degradation, but spread to secondary lymphoid organs and induce synthesis of membrane-associated pMCH-II complexes (Muntasell, Berger et al. 2007). Interestingly, follicular DCs (FDCs), which are known to release pMHC-II via exosomes (Denzer, van Eijk et al. 2000) express PrP^C on their plasma membrane and in PrP^{Sc}-infected organisms FDCs spread PrP^{Sc} from lymphoid tissue to adjacent nerve fibres that mediate prion neuroinvasion (von Poser-Klein, Flechsig et al. 2008) probably also via exosomes. PrP^C is abundantly expressed on the exosomal and plasma membrane of FDCs and suggesting a role for PrP^C in the correct transport of pMHC-II between immune cells. In fact, the formation of antigenic pMHC-II requires traffic to pre-lysosomal compartments (Watts 1997). Thus PrP^C may retain pMHC-II bearing exosomes in early endosomal compartments of the recipient cell and ensure synthesis of pMHC-II and therefor immune activation. This hypothesis is strongly supported by studies on PrP^C in adaptive immunity, showing that PrP^C expression on the plasma membrane, which

may result in higher PrP^C abundance on exosomes, is increased upon T-cell activation. Most important, they found that the activation of T-cells was much less induced (reduced induction of several T-helper-cytokines) when PrP^C was knocked out *in vitro* and *in vivo*. They suggest, "PrP^C is a potentially important molecule influencing T-cell activation and effector function" (Mabbott, Brown et al. 1997; Ingram, Isaacs et al. 2009). The results of my study suggest a very important role in immune activation for PrP^C as it may mediate retention of exosomes bearing pMHC-II in early endosomal compartments of recipient immune cells like T-cells to ensure their activation and an efficient immune response.

7.6 Outlook

This study advances understanding of the relationship of PrP^C and exosomes. It was demonstrated that PrP^C decreases the uptake of exosomes and retains exosomes in early endosomal compartments of recipient neuronal cells. A novel physiological function of PrP^C is postulated at which PrP^C mediates the internalization or the attachment of exosomes. Whether other interaction partners of PrP^C, such as LRP-1 or tetraspanins are involved in this mechanism needs to be investigated. Since PrP^C is expressed abundantly on a great variety of cell types, the function of PrP^C in exosomal internalization can help elucidating several phenotypes such as enhanced phagocytosis or reduced activation of immune response in PrP^C knockout mice. In further experiments it would be interesting to examine whether the presence of PrP^C alters the ability of exosomes to induce signalling in recipient cells. The specific mechanism of PrP^C sorting into exosomes may be examined utilizing PrP^C-mutants that lack one or two glycosylation sites or posses a shortened GPI-anchor since these mutations were shown to influence targeting to the plasma membrane and therefore might also influence the sorting of PrP^C into exosomes (Puig, Altmeppen et al. 2011). To further investigate the exosomal endocytic route fluorescently labelled PrP^C as well as fluorescently labelled exosomal marker proteins (like Tsg101 or AIP-1) would provide suitable tools. Besides the examination of specific compartments involved in the intracellular trafficking of PrP^C- and PrP$^{-/-}$- exosomes it would be interesting to identify whether PrP^C is shed from exosomes in a certain compartment or whether it will be degraded. With the use of super resolution microscopy these questions may be addressed since single fluorescent exosomes and their PrP^C content (fluorescently labelled by an antibody or after transfection of the exosomal

donor cell with fluorescently tagged PrP^C) may be visualized for several time points of endocytosis. A possible fusion of PrP^C-exosomes with PrP$^{-/-}$-recipient cells may be revealed by immuno-EM against PrP^C. If PrP^C is present on the plasma membrane of PrP$^{-/-}$-cells after endocytosis of PrP^C-exosomes it will be very likely that these exosomes, or at least some, were taken up by fusion of the membranes.

8 REFERENCES

(1982). "Scrapie: strategies, stalemates, and successes [editorial]." Lancet **1**(8283): 1221-1223.

(1991). "Origins of BSE " Vet Rec **128**(13): 310.

Abusamra, A. J., Z. Zhong, et al. (2005). "Tumor exosomes expressing Fas ligand mediate CD8+ T-cell apoptosis." Blood Cells Mol Dis **35**(2): 169-173.

Aguzzi, A. and L. Rajendran (2009). "The transcellular spread of cytosolic amyloids, prions, and prionoids." Neuron **64**(6): 783-790.

Alais, S., S. Simoes, et al. (2008). "Mouse neuroblastoma cells release prion infectivity associated with exosomal vesicles." Biol Cell **100**(10): 603-615.

Altmeppen, H. C., J. Prox, et al. (2011). "Lack of a-disintegrin-and-metalloproteinase ADAM10 leads to intracellular accumulation and loss of shedding of the cellular prion protein in vivo." Mol Neurodegener **6**: 36.

Andre, F., N. E. Schartz, et al. (2002). "Tumor-derived exosomes: a new source of tumor rejection antigens." Vaccine **20 Suppl 4**: A28-31.

Babst, M. (2005). "A protein's final ESCRT." Traffic **6**(1): 2-9.

Baier, M., S. Norley, et al. (2003). "Prion diseases: infectious and lethal doses following oral challenge." J Gen Virol **84**(Pt 7): 1927-1929.

Bessen, R. A., D. A. Kocisko, et al. (1995). "Non-genetic propagation of strain-specific properties of scrapie prion protein." Nature **375**(6533): 698-700.

Billeter, M., R. Riek, et al. (1997). "Prion protein NMR structure and species barrier for prion diseases." Proc Natl Acad Sci U S A **94**(14): 7281-7285.

Bilodeau, P. S., J. L. Urbanowski, et al. (2002). "The Vps27p Hse1p complex binds ubiquitin and mediates endosomal protein sorting." Nat Cell Biol **4**(7): 534-539.

Blott, E. J. and G. M. Griffiths (2002). "Secretory lysosomes." Nat Rev Mol Cell Biol **3**(2): 122-131.

Borchelt, D. R., A. Taraboulos, et al. (1992). "Evidence for synthesis of scrapie prion proteins in the endocytic pathway." J Biol Chem **267**(23): 16188-16199.

Brown, D. R., B. Schmidt, et al. (1998). "Prion protein expression in muscle cells and toxicity of a prion protein fragment." Eur J Cell Biol **75**(1): 29-37.

Brown, P., M. Preece, et al. (2000). "Iatrogenic Creutzfeldt-Jakob disease at the millennium." Neurology **55**(8): 1075-1081.

Bruce, M., A. Chree, et al. (1994). "Transmission of bovine spongiform encephalopathy and scrapie to mice: strain variation and the species barrier." Philos Trans R Soc Lond B Biol Sci **343**(1306): 405-411.

Bruce, M. E., R. G. Will, et al. (1997). "Transmissions to mice indicate that 'new variant' CJD is caused by the BSE agent." Nature **389**(6650): 498-501.

Bueler, H., A. Aguzzi, et al. (1993). "Mice devoid of PrP are resistant to scrapie." Cell **73**(7): 1339-1347.

Bueler, H., M. Fischer, et al. (1992). "Normal development and behaviour of mice lacking the neuronal cell-surface PrP protein." Nature **356**(6370): 577-582.

Büeler, H. R., A. Aguzzi, et al. (1993). "Mice devoid of PrP are resistant to scrapie." Cell **73**(7): 1339-1347.

Callahan, M. A., L. Xiong, et al. (2001). "Reversibility of scrapie-associated prion protein aggregation." J Biol Chem **276**(30): 28022-28028.

Calvete, J. J., D. Solis, et al. (1994). "Glycosylated boar spermadhesin AWN-1 isoforms. Biological origin, structural characterization by lectin mapping, localization of O-glycosylation sites, and effect of glycosylation on ligand binding." Biol Chem Hoppe Seyler **375**(10): 667-673.

Calzolari, A., C. Raggi, et al. (2006). "TfR2 localizes in lipid raft domains and is released in exosomes to activate signal transduction along the MAPK pathway." J Cell Sci **119**(Pt 21): 4486-4498.

Campana, V., A. Caputo, et al. (2007). "Characterization of the properties and trafficking of an anchorless form of the prion protein." J Biol Chem **282**(31): 22747-22756.

Cashman, N. R., R. Loertscher, et al. (1990). "Cellular isoform of the scrapie agent protein participates in lymphocyte activation." Cell **61**(1): 185-192.

Castilla, J., P. Saa, et al. (2005). "In vitro generation of infectious scrapie prions." Cell **121**(2): 195-206.

Caughey, B., D. A. Kocisko, et al. (1995). "Aggregates of scrapie-associated prion protein induce the cell-free conversion of protease-sensitive prion protein to the protease-resistant state." Chem Biol **2**(12): 807-817.

Caughey, B., R. Race, et al. (1989). "Comparative sequence analysis, in vitro expression and biosynthesis of mouse PrP." Prog Clin Biol Res **317**: 619-636.

Caughey, B., G. J. Raymond, et al. (2001). "Interactions and conversions of prion protein isoforms." Adv Protein Chem **57**: 139-169.

Chiesa, R., P. Piccardo, et al. (2003). "Molecular distinction between pathogenic and infectious properties of the prion protein." J Virol **77**(13): 7611-7622.

Chu, B. (1997). "Laser light scattering of polymer solutions." Appl Opt **36**(30): 7650-7656.

Cohen, A. S. (1994). "Clinical aspects of amyloidosis, including related proteins and central nervous system amyloid." Curr Opin Rheumatol **6**(1): 68-77.

Colby, D. W. and S. B. Prusiner (2011). "Prions." Cold Spring Harb Perspect Biol **3**(1): a006833.

Davis, D. M. (2007). "Intercellular transfer of cell-surface proteins is common and can affect many stages of an immune response." Nat Rev Immunol **7**(3): 238-243.

Davis, M. M., J. J. Boniface, et al. (1998). "Ligand recognition by alpha beta T cell receptors." Annu Rev Immunol **16**: 523-544.

de Almeida, C. J., L. B. Chiarini, et al. (2005). "The cellular prion protein modulates phagocytosis and inflammatory response." J Leukoc Biol **77**(2): 238-246.

de Gassart, A., C. Geminard, et al. (2003). "Lipid raft-associated protein sorting in exosomes." Blood **102**(13): 4336-4344.

Deleault, N. R., J. C. Geoghegan, et al. (2005). "Protease-resistant prion protein amplification reconstituted with partially purified substrates and synthetic polyanions." J Biol Chem **280**(29): 26873-26879.

Deleault, N. R., B. T. Harris, et al. (2007). "Formation of native prions from minimal components in vitro." Proc Natl Acad Sci U S A **104**(23): 9741-9746.

Denzer, K., M. van Eijk, et al. (2000). "Follicular dendritic cells carry MHC class II-expressing microvesicles at their surface." J Immunol **165**(3): 1259-1265.

Dermine, J. F., S. Duclos, et al. (2001). "Flotillin-1-enriched lipid raft domains accumulate on maturing phagosomes." J Biol Chem **276**(21): 18507-18512.

Dodelet, V. C. and N. R. Cashman (1998). "Prion protein expression in human leukocyte differentiation." Blood **91**(5): 1556-1561.

Durig, J., A. Giese, et al. (2000). "Differential constitutive and activation-dependent expression of prion protein in human peripheral blood leucocytes." Br J Haematol **108**(3): 488-495.

Ecroyd, H., P. Sarradin, et al. (2004). "Compartmentalization of prion isoforms within the reproductive tract of the ram." Biol Reprod **71**(3): 993-1001.

Faure, J., G. Lachenal, et al. (2006). "Exosomes are released by cultured cortical neurones." Mol Cell Neurosci **31**(4): 642-648.

Feng, D., W. L. Zhao, et al. (2010). "Cellular internalization of exosomes occurs through phagocytosis." Traffic **11**(5): 675-687.

Fevrier, B. and G. Raposo (2004). "Exosomes: endosomal-derived vesicles shipping extracellular messages." Current Opinion in Cell Biology **16**(4): 415-421.

Fevrier, B., D. Vilette, et al. (2004). "Cells release prions in association with exosomes." Proc Natl Acad Sci U S A **101**(26): 9683-9688.

Fischer, M., T. Rulicke, et al. (1996). "Prion protein (PrP) with amino-proximal deletions restoring susceptibility of PrP knockout mice to scrapie." EMBO J **15**(6): 1255-1264.

Fitzner, D., M. Schnaars, et al. (2011). "Selective transfer of exosomes from oligodendrocytes to microglia by macropinocytosis." J Cell Sci **124**(Pt 3): 447-458.

Ford, M. J., L. J. Burton, et al. (2002). "A marked disparity between the expression of prion protein and its message by neurones of the CNS." Neuroscience **111**(3): 533-551.

Gajdusek, D. C. (1988). "Transmissible and non-transmissible amyloidoses: autocatalytic post-translational conversion of host precursor proteins to beta-pleated sheet configurations." J Neuroimmunol **20**(2-3): 95-110.

Gambetti, P., Z. Dong, et al. (2008). "A novel human disease with abnormal prion protein sensitive to protease." Ann Neurol **63**(6): 697-708.

Gastpar, R., M. Gehrmann, et al. (2005). "Heat shock protein 70 surface-positive tumor exosomes stimulate migratory and cytolytic activity of natural killer cells." Cancer Res **65**(12): 5238-5247.

Glatzel, M. and A. Aguzzi (2000). "PrP(C) expression in the peripheral nervous system is a determinant of prion neuroinvasion." J Gen Virol **81**(Pt 11): 2813-2821.

Gousset, K., E. Schiff, et al. (2009). "Prions hijack tunnelling nanotubes for intercellular spread." Nat Cell Biol **11**(3): 328-336.

Gruenberg, J. and H. Stenmark (2004). "The biogenesis of multivesicular endosomes." Nat Rev Mol Cell Biol **5**(4): 317-323.

Hamir, A. N., R. C. Cutlip, et al. (2001). "Preliminary findings on the experimental transmission of chronic wasting disease agent of mule deer to cattle." J Vet Diagn Invest **13**(1): 91-96.

Haraguchi, T., S. Fisher, et al. (1989). "Asparagine-linked glycosylation of the scrapie and cellular prion proteins." Arch Biochem Biophys **274**(1): 1-13.

Hay, B., R. A. Barry, et al. (1987). "Biogenesis and transmembrane orientation of the cellular isoform of the scrapie prion protein [published errratum appears in Mol Cell Biol 1987 May;7(5):2035]." Mol Cell Biol **7**(2): 914-920.

Hill, A. F., R. J. Butterworth, et al. (1999). "Investigation of variant Creutzfeldt-Jakob disease and other human prion diseases with tonsil biopsy samples." Lancet **353**(9148): 183-189.

Hill, A. F., M. Desbruslais, et al. (1997). "The same prion strain causes vCJD and BSE." Nature **389**(6650): 448-450, 526.

Hofmann, K. and L. Falquet (2001). "A ubiquitin-interacting motif conserved in components of the proteasomal and lysosomal protein degradation systems." Trends Biochem Sci **26**(6): 347-350.

Hood, J. L., H. Pan, et al. (2009). "Paracrine induction of endothelium by tumor exosomes." Lab Invest **89**(11): 1317-1328.

Horiuchi, M., N. Yamazaki, et al. (1995). "A cellular form of prion protein (PrPC) exists in many non-neuronal tissues of sheep." J Gen Virol **76 (Pt 10)**: 2583-2587.

Hsiao, K., H. F. Baker, et al. (1989). "Linkage of a prion protein missense variant to Gerstmann-Straussler syndrome." Nature **338**(6213): 342-345.

Hsiao, K., M. Scott, et al. (1991). "Spontaneous neurodegeneration in transgenic mice with prion protein codon 101 proline----leucine substitution." Ann N Y Acad Sci **640**: 166-170.

Hsiao, K. K. (1994). "The genetics and transgenetics of human prion disease." Ann N Y Acad Sci **724**: 241-245.

Huang, Z., J. M. Gabriel, et al. (1994). "Proposed three-dimensional structure for the cellular prion protein." Proc Natl Acad Sci U S A **91**(15): 7139-7143.

Hunter, N., J. Foster, et al. (2002). "Transmission of prion diseases by blood transfusion." J Gen Virol **83**(Pt 11): 2897-2905.

Ingram, R. J., J. D. Isaacs, et al. (2009). "A role of cellular prion protein in programming T-cell cytokine responses in disease." FASEB J **23**(6): 1672-1684.

James, T. L., H. Liu, et al. (1997). "Solution structure of a 142-residue recombinant prion protein corresponding to the infectious fragment of the scrapie isoform." Proc Natl Acad Sci U S A **94**(19): 10086-10091.

Jarrett, J. T. and P. T. Lansbury, Jr. (1993). "Seeding "one-dimensional crystallization" of amyloid: a pathogenic mechanism in Alzheimer's disease and scrapie?" Cell **73**(6): 1055-1058.

Jen, A., C. J. Parkyn, et al. (2010). "Neuronal low-density lipoprotein receptor-related protein 1 binds and endocytoses prion fibrils via receptor cluster 4." J Cell Sci **123**(Pt 2): 246-255.

Johnson, R. T. (2005). "Prion diseases." Lancet Neurol **4**(10): 635-642.

Kaneko, K., L. Zulianello, et al. (1997). "Evidence for protein X binding to a discontinuous epitope on the cellular prion protein during scrapie prion propagation." Proc Natl Acad Sci U S A **94**(19): 10069-10074.

Kim, S. H., N. Bianco, et al. (2006). "Exosomes derived from genetically modified DC expressing FasL are anti-inflammatory and immunosuppressive." Mol Ther **13**(2): 289-300.

Kim, S. H., E. R. Lechman, et al. (2005). "Exosomes derived from IL-10-treated dendritic cells can suppress inflammation and collagen-induced arthritis." J Immunol **174**(10): 6440-6448.

Klatzo, I., D. C. Gajdusek, et al. (1959). "Pathology of Kuru." Lab Invest **8**(4): 799-847.

Kocisko, D. A., J. H. Come, et al. (1994). "Cell-free formation of protease-resistant prion protein." Nature **370**(6489): 471-474.

Kogure, T., W. L. Lin, et al. (2011). "Intercellular nanovesicle-mediated microRNA transfer: A mechanism of environmental modulation of hepatocellular cancer cell growth." Hepatology.

Kovacs, G. G., R. Hoftberger, et al. (2005). "Neuropathology of white matter disease in Leber's hereditary optic neuropathy." Brain **128**(Pt 1): 35-41.

Kramer-Albers, E. M., N. Bretz, et al. (2007). "Oligodendrocytes secrete exosomes containing major myelin and stress-protective proteins: Trophic support for axons?" Proteomics Clin Appl **1**(11): 1446-1461.

Kubosaki, A., S. Yusa, et al. (2001). "Distribution of cellular isoform of prion protein in T lymphocytes and bone marrow, analyzed by wild-type and prion protein gene-deficient mice." Biochem Biophys Res Commun **282**(1): 103-107.

Leblanc, P., S. Alais, et al. (2006). "Retrovirus infection strongly enhances scrapie infectivity release in cell culture." Embo J **25**(12): 2674-2685.

Legname, G., I. V. Baskakov, et al. (2004). "Synthetic mammalian prions." Science **305**(5684): 673-676.

Legname, G., H. O. Nguyen, et al. (2005). "Strain-specified characteristics of mouse synthetic prions." Proc Natl Acad Sci U S A **102**(6): 2168-2173.

Li, R., D. Liu, et al. (2001). "The expression and potential function of cellular prion protein in human lymphocytes." Cell Immunol **207**(1): 49-58.

Liu, T., R. Li, et al. (2002). "Intercellular transfer of the cellular prion protein." J Biol Chem **277**(49): 47671-47678.

Lloyd, S. E., O. N. Onwuazor, et al. (2001). "Identification of multiple quantitative trait loci linked to prion disease incubation period in mice." Proc Natl Acad Sci U S A **98**(11): 6279-6283.

Mabbott, N. A., K. L. Brown, et al. (1997). "T-lymphocyte activation and the cellular form of the prion protein." Immunology **92**(2): 161-165.

Mackay, G. A., R. S. Knight, et al. (2011). "The molecular epidemiology of variant CJD." Int J Mol Epidemiol Genet **2**(3): 217-227.

Magalhaes, A. C., G. S. Baron, et al. (2005). "Uptake and neuritic transport of scrapie prion protein coincident with infection of neuronal cells." J Neurosci **25**(21): 5207-5216.

Maglio, L. E., M. F. Perez, et al. (2004). "Hippocampal synaptic plasticity in mice devoid of cellular prion protein." Brain Res Mol Brain Res **131**(1-2): 58-64.

Mallucci, G. R., T. A. Campbell, et al. (1999). "Inherited prion disease with an alanine to valine mutation at codon 117 in the prion protein gene." Brain **122 (Pt 10)**: 1823-1837.

Manolakou, K., J. Beaton, et al. (2001). "Genetic and environmental factors modify bovine spongiform encephalopathy incubation period in mice." Proc Natl Acad Sci U S A **98**(13): 7402-7407.

Manson, J., J. D. West, et al. (1992). "The prion protein gene: a role in mouse embryogenesis?" Development **115**(1): 117-122.

Marijanovic, Z., A. Caputo, et al. (2009). "Identification of an intracellular site of prion conversion." PLoS Pathog **5**(5): e1000426.

Mathews, J. A., D. R. Gibb, et al. (2010). "CD23 Sheddase A disintegrin and metalloproteinase 10 (ADAM10) is also required for CD23 sorting into B cell-derived exosomes." J Biol Chem **285**(48): 37531-37541.

McKnight, T. D., D. C. Alexander, et al. (1986). "Nucleotide sequence and molecular evolution of two tomato genes encoding the small subunit of ribulose-1,5-bisphosphate carboxylase." Gene **48**(1): 23-32.

Miesbauer, M., A. S. Rambold, et al. (2010). "Targeting of the prion protein to the cytosol: mechanisms and consequences." Curr Issues Mol Biol **12**(2): 109-118.

Morelli, A. E., A. T. Larregina, et al. (2004). "Endocytosis, intracellular sorting, and processing of exosomes by dendritic cells." Blood **104**(10): 3257-3266.

Morris, R. J., C. J. Parkyn, et al. (2006). "Traffic of prion protein between different compartments on the neuronal surface, and the propagation of prion disease." FEBS Lett **580**(23): 5565-5571.

Muntasell, A., A. C. Berger, et al. (2007). "T cell-induced secretion of MHC class II-peptide complexes on B cell exosomes." EMBO J **26**(19): 4263-4272.

Nico, P. B., F. de-Paris, et al. (2005). "Altered behavioural response to acute stress in mice lacking cellular prion protein." Behav Brain Res **162**(2): 173-181.

Nishida, N., S. Katamine, et al. (1997). "Prion protein is necessary for latent learning and long-term memory retention." Cell Mol Neurobiol **17**(5): 537-545.

Nitta, K., A. Sakudo, et al. (2009). "Role of cellular prion proteins in the function of macrophages and dendritic cells." Protein Pept Lett **16**(3): 239-246.

Nolte-'t Hoen, E. N., S. I. Buschow, et al. (2009). "Activated T cells recruit exosomes secreted by dendritic cells via LFA-1." Blood **113**(9): 1977-1981.

Oh, J. M., H. Y. Shin, et al. (2008). "The involvement of cellular prion protein in the autophagy pathway in neuronal cells." Mol Cell Neurosci **39**(2): 238-247.

Parkyn, C. J., E. G. Vermeulen, et al. (2008). "LRP1 controls biosynthetic and endocytic trafficking of neuronal prion protein." J Cell Sci **121**(Pt 6): 773-783.

Parolini, I., C. Federici, et al. (2009). "Microenvironmental pH is a key factor for exosome traffic in tumor cells." J Biol Chem **284**(49): 34211-34222.

Peden, A. H., M. W. Head, et al. (2004). "Preclinical vCJD after blood transfusion in a PRNP codon 129 heterozygous patient." Lancet **364**(9433): 527-529.

Piper, R. C. and D. J. Katzmann (2007). "Biogenesis and function of multivesicular bodies." Annu Rev Cell Dev Biol **23**: 519-547.

Piper, R. C. and J. P. Luzio (2001). "Late endosomes: sorting and partitioning in multivesicular bodies." Traffic **2**(9): 612-621.

Pisitkun, T., R. F. Shen, et al. (2004). "Identification and proteomic profiling of exosomes in human urine." Proc Natl Acad Sci U S A **101**(36): 13368-13373.

Pornillos, O., S. L. Alam, et al. (2002). "Structure and functional interactions of the Tsg101 UEV domain." EMBO J **21**(10): 2397-2406.

Porto-Carreiro, I., B. Fevrier, et al. (2005). "Prions and exosomes: from PrPc trafficking to PrPsc propagation." Blood Cells Mol Dis **35**(2): 143-148.

Prusiner, S. B. (1989). "Creutzfeldt-Jakob disease and scrapie prions." Alzheimer Dis Assoc Disord **3**(1-2): 52-78.

Prusiner, S. B. (2001). "Shattuck lecture--neurodegenerative diseases and prions." N Engl J Med **344**(20): 1516-1526.

Prusiner, S. B. and M. R. Scott (1997). "Genetics of prions." Annu Rev Genet **31**: 139-175.

Prusiner, S. B., M. R. Scott, et al. (1998). "Prion protein biology." Cell **93**(3): 337-348.

Puig, B., H. C. Altmeppen, et al. (2011). "N-glycans and glycosylphosphatidylinositol-anchor act on polarized sorting of mouse PrP(C) in Madin-Darby canine kidney cells." PLoS One **6**(9): e24624.

Raeber, A. J., A. Sailer, et al. (1999). "Ectopic expression of prion protein (PrP) in T lymphocytes or hepatocytes of PrP knockout mice is insufficient to sustain prion replication." Proc Natl Acad Sci U S A **96**(7): 3987-3992.

Raiborg, C., K. G. Bache, et al. (2002). "Hrs sorts ubiquitinated proteins into clathrin-coated microdomains of early endosomes." Nat Cell Biol **4**(5): 394-398.

Raiborg, C., T. E. Rusten, et al. (2003). "Protein sorting into multivesicular endosomes." Curr Opin Cell Biol **15**(4): 446-455.

Ramachandran, S. and V. Palanisamy (2011). "Horizontal transfer of RNAs: exosomes as mediators of intercellular communication." Wiley Interdiscip Rev RNA.

Rani, S., K. O'Brien, et al. (2011). "Isolation of exosomes for subsequent mRNA, MicroRNA, and protein profiling." Methods Mol Biol **784**: 181-195.

Raymond, G. J., J. Hope, et al. (1997). "Molecular assessment of the potential transmissibilities of BSE and scrapie to humans." Nature **388**(6639): 285-288.

Reggiori, F. and H. R. Pelham (2001). "Sorting of proteins into multivesicular bodies: ubiquitin-dependent and -independent targeting." EMBO J **20**(18): 5176-5186.

Riek, R., S. Hornemann, et al. (1996). "NMR structure of the mouse prion protein domain PrP(121-231)." Nature **382**(6587): 180-182.

Riek, R., G. Wider, et al. (1998). "Prion protein NMR structure and familial human spongiform encephalopathies." Proc Natl Acad Sci U S A **95**(20): 11667-11672.

Robertson, C., S. A. Booth, et al. (2006). "Cellular prion protein is released on exosomes from activated platelets." Blood **107**(10): 3907-3911.

Roos, R., D. C. Gajdusek, et al. (1973). "The clinical characteristics of transmissible Creutzfeldt-Jakob disease." Brain **96**(1): 1-20.

Saborio, G. P., C. Soto, et al. (1999). "Cell-lysate conversion of prion protein into its protease-resistant isoform suggests the participation of a cellular chaperone." Biochem Biophys Res Commun **258**(2): 470-475.

Safar, J. G., P. Lessard, et al. (2008). "Transmission and detection of prions in feces." J Infect Dis **198**(1): 81-89.

Segura, E., S. Amigorena, et al. (2005). "Mature dendritic cells secrete exosomes with strong ability to induce antigen-specific effector immune responses." Blood Cells Mol Dis **35**(2): 89-93.

Segura, E., C. Nicco, et al. (2005). "ICAM-1 on exosomes from mature dendritic cells is critical for efficient naive T-cell priming." Blood **106**(1): 216-223.

Silveira, J. R., G. J. Raymond, et al. (2005). "The most infectious prion protein particles." Nature **437**(7056): 257-261.

Silverman, J. M., J. Clos, et al. (2010). "An exosome-based secretion pathway is responsible for protein export from Leishmania and communication with macrophages." J Cell Sci **123**(Pt 6): 842-852.

Simons, K. and E. Ikonen (1997). "Functional rafts in cell membranes." Nature **387**(6633): 569-572.

Simons, M. and G. Raposo (2009). "Exosomes--vesicular carriers for intercellular communication." Curr Opin Cell Biol **21**(4): 575-581.

Skog, J., T. Wurdinger, et al. (2008). "Glioblastoma microvesicles transport RNA and proteins that promote tumour growth and provide diagnostic biomarkers." Nat Cell Biol **10**(12): 1470-1476.

Sokolova, V., A. K. Ludwig, et al. (2011). "Characterisation of exosomes derived from human cells by nanoparticle tracking analysis and scanning electron microscopy." Colloids Surf B Biointerfaces **87**(1): 146-150.

Spielhaupter, C. and H. M. Schatzl (2001). "PrPC directly interacts with proteins involved in signaling pathways." J Biol Chem **276**(48): 44604-44612.

Steelman, V. M. (1994). "Creutzfeld-Jakob disease: recommendations for infection control." Am J Infect Control **22**(5): 312-318.

Stekel, D. J., M. A. Nowak, et al. (1996). "Prediction of future BSE spread." Nature **381**(6578): 119.

Stephenson, D. A., K. Chiotti, et al. (2000). "Quantitative trait loci affecting prion incubation time in mice." Genomics **69**(1): 47-53.

Stimson, E., J. Hope, et al. (1999). "Site-specific characterization of the N-linked glycans of murine prion protein by high-performance liquid chromatography/electrospray mass spectrometry and exoglycosidase digestions." Biochemistry **38**(15): 4885-4895.

Stoeck, A., S. Keller, et al. (2006). "A role for exosomes in the constitutive and stimulus-induced ectodomain cleavage of L1 and CD44." Biochem J **393**(Pt 3): 609-618.

Stohr, J., K. Elfrink, et al. (2011). "In vitro conversion and seeded fibrillization of posttranslationally modified prion protein." Biol Chem **392**(5): 415-421.

Stoorvogel, W., M. J. Kleijmeer, et al. (2002). "The biogenesis and functions of exosomes." Traffic **3**(5): 321-330.

Stoorvogel, W., G. J. Strous, et al. (1991). "Late endosomes derive from early endosomes by maturation." Cell **65**(3): 417-427.

Sullivan, R., F. Saez, et al. (2005). "Role of exosomes in sperm maturation during the transit along the male reproductive tract." Blood Cells Mol Dis **35**(1): 1-10.

Sunyach, C., A. Jen, et al. (2003). "The mechanism of internalization of glycosylphosphatidylinositol-anchored prion protein." EMBO J **22**(14): 3591-3601.

Telling, G. C., M. Scott, et al. (1995). "Prion propagation in mice expressing human and chimeric PrP transgenes implicates the interaction of cellular PrP with another protein." Cell **83**(1): 79-90.

Testa, J. S., G. S. Apcher, et al. (2010). "Exosome-driven antigen transfer for MHC class II presentation facilitated by the receptor binding activity of influenza hemagglutinin." J Immunol **185**(11): 6608-6616.

Thery, C., M. Boussac, et al. (2001). "Proteomic analysis of dendritic cell-derived exosomes: a secreted subcellular compartment distinct from apoptotic vesicles." J Immunol **166**(12): 7309-7318.

Thery, C., L. Duban, et al. (2002). "Indirect activation of naive CD4+ T cells by dendritic cell-derived exosomes." Nat Immunol **3**(12): 1156-1162.

Thery, C., M. Ostrowski, et al. (2009). "Membrane vesicles as conveyors of immune responses." Nat Rev Immunol **9**(8): 581-593.

Thery, C., L. Zitvogel, et al. (2002). "Exosomes: composition, biogenesis and function." Nat Rev Immunol **2**(8): 569-579.

Tobler, I., S. E. Gaus, et al. (1996). "Altered circadian activity rhythms and sleep in mice devoid of prion protein." Nature **380**(6575): 639-642.

Vella, L. J., D. L. Greenwood, et al. (2008). "Enrichment of prion protein in exosomes derived from ovine cerebral spinal fluid." Vet Immunol Immunopathol **124**(3-4): 385-393.

Vella, L. J. and A. F. Hill (2008). "Generation of cell lines propagating infectious prions and the isolation and characterization of cell-derived exosomes." Methods Mol Biol **459**: 69-82.

Vella, L. J., R. A. Sharples, et al. (2007). "Packaging of prions into exosomes is associated with a novel pathway of PrP processing." J Pathol **211**(5): 582-590.

Vella, L. J., R. A. Sharples, et al. (2008). "The role of exosomes in the processing of proteins associated with neurodegenerative diseases." Eur Biophys J **37**(3): 323-332.

von Poser-Klein, C., E. Flechsig, et al. (2008). "Alteration of B-cell subsets enhances neuroinvasion in mouse scrapie infection." J Virol **82**(7): 3791-3795.

von Zastrow, M. and A. Sorkin (2007). "Signaling on the endocytic pathway." Curr Opin Cell Biol **19**(4): 436-445.

Wadia, J. S., M. Schaller, et al. (2008). "Pathologic prion protein infects cells by lipid-raft dependent macropinocytosis." PLoS One **3**(10): e3314.

Wang, G., X. Zhou, et al. (2010). "Cellular prion protein released on exosomes from macrophages binds to Hsp70." Acta Biochim Biophys Sin (Shanghai) **42**(5): 345-350.

Watts, C. (1997). "Capture and processing of exogenous antigens for presentation on MHC molecules." Annu Rev Immunol **15**: 821-850.

Weissmann, C. (1991). "Spongiform encephalopathies. The prion's progress." Nature **349**(6310): 569-571.

Wender, P. A., D. J. Mitchell, et al. (2000). "The design, synthesis, and evaluation of molecules that enable or enhance cellular uptake: peptoid molecular transporters." Proc Natl Acad Sci U S A **97**(24): 13003-13008.

Wille, H., M. A. Baldwin, et al. (1996). "Prion protein amyloid: separation of scrapie infectivity from PrP polymers." Ciba Found Symp **199**: 181-199; discussion 199-201.

Wubbolts, R., R. S. Leckie, et al. (2003). "Proteomic and biochemical analyses of human B cell-derived exosomes. Potential implications for their function and multivesicular body formation." J Biol Chem **278**(13): 10963-10972.

Zahn, R., A. Liu, et al. (2000). "NMR solution structure of the human prion protein." Proc Natl Acad Sci U S A **97**(1): 145-150.

Zitvogel, L., A. Regnault, et al. (1998). "Eradication of established murine tumors using a novel cell-free vaccine: dendritic cell-derived exosomes." Nat Med **4**(5): 594-600.

Zomer, A., T. Vendrig, et al. (2010). "Exosomes: Fit to deliver small RNA." Commun Integr Biol **3**(5): 447-450.

9 APPENDIX

9.1 List of abbreviations

AA	Amino acid
AD	Alzheimer`s disease
ADAM10	A-Disentegrin-And-Metalloproteinase10
AIP-1	ALG-2-Interacting protein
APP	Amyloid precursor protein
APS	Ammoniumpersulfat
AraC	Cytosine Arabinoside
BSE	Bovine spongiform encephalopathy
CC	Charged core
CJD	Creutzfeldt-Jakob disease
CL	Cell line
CNS	Central nerve system
CR	Count rate
CSF	Cerebral spinal fluid
CWD	Chronic wasting disease
DAPI	4',6-diamidino-2-phenylindole
DC	Dendritic cell
DLS	Dynamic light scattering
DMSO	Dimethylsulfoxide
DNA	Deoxyribonucleic acid
E14	Embryonic day 14
ED	Exosome donor
EDTA	Ethylenediaminetreaceticacid
EM	Electron microscopy
EP	Exosomal pellet
ER	Exosome recipient
ESCRT	Endosomal sorting complex required for transport
FACS	Fluorescence Activated Cell Sorting
gCJD	genetic Creutzfeldt-Jakob disease
FCS	Fetal Calf Serum

FDC	Follicular dendritic cells
FFI	Fatal Familial Insomnia
GPI	Glycosylphosphatidylinositol
4-(2-Hydroxyethyl)piperazine -1-ethanesulfonic acid	HEPES
GM130	Golgi marker protein 130
GSS	Gerstmann-Sträussler-Scheinker syndrom
h	hour
HC	Hydrophobic core
HS	Horse Serum
ICAM-1	Intercellular adhesion molecule 1
IF	Immunofluorescence
ILV	Intraluminal vesicle
LBPA	Lysobisphosphatidic acid
LR	Laminin receptor
LRP	Low-density lipoprotein receptor-related protein1
MHC-II	Major histocompatibility complex II
min	minute
MVB	Multivesicular body
MVE	Multivesicular endosome
NEUpA	Numeric exosomal uptake assay
OR	Octarepeat
PAGE	Polyacrylamide gel electrophoresis
PBS	Phosphate buffered saline
PI	Proteinase inhibitor
PLL	Poly-L-Lysin
PN	Primary neurons
PrP	Prion protein
PrP^C	Prion Protein cellular
PrP^{Sc}	Prion Protein scrapie
PrP^{3F4}	Prion Protein 3F4 tagged
$PrP^{-/-}$	Prion Protein knockout
$PrP^{0/0}$	Prion Protein knockout mouse
P/S	Penicillin/Streptomycin

RK13	Rabbit kidney epithelial
RNA	Ribonucleic acid
RT	Room temperature
sCJD	Sporadic Creutzfeldt-Jakob disease
SDS	Sodiumdodecylsulfate
sec	second
SLS	Static light scattering
SP	Signal peptide
Stdv.	Standard deviation
TEMED	Tetramethylendiamine
TCR	T-cell receptor
Tfr	Transferrin
TGN	Trans-golgi network
TME	Transmissible mink encephalopathy
TSE	Transmissible spongiform encephalopathy
Tsg101	Tumor susceptibility gene101
UEV	Ubiquitin E2 variant
UIM	Ubiquitin-interacting motif
WB	Western blot
Wt	wild type

9.2 List of figures

9.3 List of tables

10 ACKNOWLEDGEMENTS

First I would like to thank Prof. Markus Glatzel for the opportunity to work in his lab and establish my PhD thesis. Thank you for supporting the project and my scientific education. Second, I thank PD Dr. Lüthje for being the second reviewer of my dissertation and I also want to thank the disputation committee for kindly accepting to evaluate my thesis.

Next, I want to thank my collaborators Dr. Lars Redecke whose interest in exosomes and cooperativeness were of great impact for the project and Prof. Derek Toomre for the opportunity to work in his lab during my internship and learn about microscopy.

Of course I thank the whole team working in the lab of Markus Glatzel and specifically the other PhD students for the great atmosphere and the perfect amount of sarcasm when needed. Especially I want to thank the "Prion-Group" Dr. Susanne Krasemann, Dr. Berta Puig, Hermann C. Altmeppen, Jan Paul Lüpke, and Kirstin Albers for their help within my project. In particular I thank Dr. Berta Puig for being a great mentor and friend.

Additionally, I want to thank Prof. Braulke and the members of the graduate school (GRK1459) for great retreats with a lot of scientific input and for establishing a wonderful symposium. Special thanks to Caro, Uli, and Vanessa; you became great friends and I thank you for the fun times and your support!

Abel, I thank you so much for your great scientific and private encouragement. You are most important to me and I am excited to take the next roads with you.

Most of all, I thank my parents for their unconditional trust and appreciation and for supporting my education.